

STUDIES FOR DETERMINING RAPID THRUST RESPONSE  
REQUIREMENTS AND  
TECHNIQUES FOR USE IN A  
LONG RANGE TRANSPORT AIRCRAFT

by

D. M. Newirth

and

W. W. Ferguson

PRATT & WHITNEY AIRCRAFT  
DIVISION OF  
UNITED AIRCRAFT CORPORATION

prepared for

NATIONAL AERONAUTICS AND SPACE ADMINISTRATION

NASA Lewis Research Center  
Contract NAS3-15550

Robert J. Antl, Project Manager

**CASE FILE  
COPY**

## NOTICE

This report was prepared as an account of Government-sponsored work. Neither the United States, nor the National Aeronautics and Space Administration (NASA), nor any person acting on behalf of NASA:

- A.) Makes any warranty or representation, expressed or implied, with respect to the accuracy, completeness, or usefulness of the information contained in this report, or that the use of any information, apparatus, method, or process disclosed in this report may not infringe privately-owned rights; or
- B.) Assumes any liabilities with respect to the use of, or for damages resulting from the use of, any information, apparatus, method or process disclosed in this report.

As used above, "person acting on behalf of NASA" includes any employee or contractor of NASA, or employee of such contractor, to the extent that such employee or contractor of NASA or employee of such contractor prepares, disseminates, or provides access to any information pursuant to his employment or contract with NASA, or his employment with such contractor.

Requests for copies of this report should be referred to

National Aeronautics and Space Administration  
Scientific and Technical Information Facility  
P.O. Box 33  
College Park, Md. 20740

1. Report No. <b>NASA CR-121243</b>		2. Government Accession No.		3. Recipient's Catalog No.	
4. Title and Subtitle <b>Studies for Determining Rapid Thrust Response Requirements and Techniques For Use in a Long Range Transport Aircraft – Exhibit A, Part II, Task II Final</b>				5. Report Date <b>August, 1973</b>	
				6. Performing Organization Code	
7. Author(s) <b>D. M. Newirth, W. W. Ferguson</b>				8. Performing Organization Report No. <b>PWA-4693</b>	
9. Performing Organization Name and Address <b>Pratt &amp; Whitney Aircraft Division of United Aircraft Corporation East Hartford, Conn. 06108</b>				10. Work Unit No.	
				11. Contract or Grant No. <b>NAS3-15550</b>	
12. Sponsoring Agency Name and Address <b>National Aeronautics and Space Administration Washington, D. C. 20546</b>				13. Type of Report and Period Covered <b>Contractor Report</b>	
				14. Sponsoring Agency Code	
15. Supplementary Notes <b>Project Manager, Robert J. Antl, V/STOL and Noise Division NASA – Lewis Research Center, Cleveland, Ohio</b>					
16. Abstract  <p>Propulsion systems proposed for the next generation of long-range transport aircraft will utilize advanced technology to reduce the noise to levels that will be inoffensive to the community. Additional reductions can be realized by adopting steeper glide slopes during the landing approach. The aircraft dynamic characteristics and methods of obtaining rapid engine response during the go-around maneuver from an aborted landing approach are identified and discussed. The study concludes that the present levels of flight safety will not be compromised by the steeper approach.</p>					
17. Key Words (Suggested by Author(s)) <b>Turbofan Engines      Thrust Response Subsonic Aircraft Advanced Technology Noise</b>				18. Distribution Statement <b>Unclassified - limited</b>	
19. Security Classif. (of this report) <b>Unclassified</b>		20. Security Classif. (of this page) <b>Unclassified</b>		21. No. of Pages <b>65</b>	
				22. Price* <b>\$3.00</b>	

\* For sale by the National Technical Information Service, Springfield, Virginia 22151

## FOREWORD

The work described herein, which was conducted by the Pratt & Whitney Aircraft Division of United Aircraft Corporation, was performed under NASA Project Manager, Mr. Robert J. Antl, V/STOL and Noise Division, NASA-Lewis Research Center. This report was prepared by D.M. Newirth and W. W. Ferguson, with contributions from K. B. Loftus, and R. Cronin, under the direction of G. L. Brines, the Pratt & Whitney Aircraft Program Manager.

The provisions of NASA Policy Directive (NPD) 2220.4, dated May 15, 1970, subject: Use of International System of Units (SI) in NASA Publications, have been waived under authority of subparagraph 5.5, NPD 2220.4.

## TABLE OF CONTENTS

	Page
SUMMARY	1
INTRODUCTION	3
AIRCRAFT DYNAMIC RESPONSE	3
RAPID ENGINE RESPONSE	21
Basic Control System	21
Rapid Response Schemes - Introduction	22
CONCLUSIONS and RECOMMENDATIONS	37
LIST OF SYMBOLS	38
DISTRIBUTION LIST	40

## LIST OF ILLUSTRATIONS

Figure	Title	Page
1	Approach Landing Go-Around	6
2	Free Body Diagram	6
3	Thrust Response Characteristics	7
4	Engine Response Time	7
5	Low Speed Aerodynamics Characteristics	9
6	Effect of Engine Response Time on Flight Profile	9
7	Effect of Engine Response Time and Approach Speed on Velocity History	10
8	Effect of Engine Response Time and Approach Speed on Velocity History	11
9	Effect of Engine Response Time and Approach Speed on Velocity History	12
10	Effect of Glide Slope Angle on Velocity History and Required Response	13
11	Component Forces Along the Flight Path	14
12	Component Forces Along the Flight Path	15
13	All Engines Operating	16
14	Total Altitude Loss	18
15	Total Altitude Loss	19
16	One Engine Inoperative	20
17	Summary of Engine Response Requirements ~ ATT Mach 0.9 Aircraft	20
18	STF 433 Engine and Fuel Control Acceleration Characteristics ~ Basic Control	21
19	Steady-State Rematch with Compressor Bleeds ~ 6° Approach	23

## LIST OF ILLUSTRATIONS (Cont'd)

Figure	Title	Page
20	Steady-State Rematch with Variable Duct Area (AJD) $\sim 6^\circ$ Approach	24
21	Variable Duct Area $\sim 6^\circ$ Approach	25
22	Transient Rematch with Variable Duct Area (AJD) $\sim 6^\circ$ Approach	25
23	Steady-State Rematch with Duct Bleeds $\sim 6^\circ$ Approach	26
24	Steady-State Rematch with Duct Bleeds $\sim 6^\circ$ Approach	27
25	Steady-State Rematch with Engine Area (AJE) $\sim 6^\circ$ Approach	27
26	Steady-State Rematch with Flow Blockage in the Inlet $\sim 6^\circ$ Approach	29
27	Steady-State Rematch with High Pressure Compressor Stator Vanes $\sim 6^\circ$ Approach	29
28	Compressor Stator Vane Rematch $\sim 6^\circ$ Approach	30
29	Steady-State Rematch with High Pressure Turbine Inlet Area $\sim 6^\circ$ Approach	30
30	Steady-State Rematch with Low Pressure Turbine Inlet Area $\sim 6^\circ$ Approach	31
31	Low Pressure Turbine Area Rematch $\sim 6^\circ$ Approach	32
32	Modified Control Logic	33
33	Modified Control Logic $\sim 6^\circ$ Approach	33
34	Combining Modified Control Logic and Stator Vane Reset $\sim 6^\circ$ Approach	34
35	Combining Modified Control Logic and Variable Low Pressure Turbine Area $\sim 6^\circ$ Approach	35
36	Combining Modified Control Logic, Stator Vane Reset and Variable Low Pressure Turbine Area $\sim 6^\circ$ Approach	35
37	Summary of Promising Schemes	36

## SUMMARY

*The purpose of this study was to investigate the thrust response requirements of the engine studied under the original NASA Lewis Research Center Contract NAS3-15550 and to investigate various methods of achieving rapid thrust response to facilitate steep approaches for noise abatement purposes.*

*The engine thrust response requirements were determined as a function of approach glide slope angle, using a dynamic simulation of a typical Advanced Technology Transport (ATT) aircraft.*

*In order to determine the necessary engine response characteristics, a parametric evaluation of various approach conditions was conducted. The evaluation included the effects of:*

- *Approach speed variations*
- *Maximum angle of attack variations*
- *Glide slope angle variations*
- *One engine inoperative considerations*
- *Speed change considerations*

*A "three degree of freedom" simulation was assumed, to evaluate the aircraft response during the execution of a missed approach maneuver.*

*The evaluation showed that the use of steeper approach glide slopes did not result in a more stringent requirement on thrust response than that required by a conventional ( $3^\circ$ ) approach. The use of steeper approach glide slope actually permits a slower responding engine.*

*The evaluation was structured such that the missed approach maneuver was considered terminated where a positive climb gradient was established. Under this constraint, the increased glide slope requires the velocity vector of the aircraft to be turned through a larger angle. Since the rotation rate of the aircraft is largely independent of engine thrust, for a fixed aircraft the larger angle change requires a longer time to complete, resulting in reduced engine response requirements.*

*Rapid engine response schemes were investigated using the P&WA<sup>TM</sup> State-of-the-Art Performance Program (SOAPP)-transient simulation of the STF433 study engine. The simulation incorporated the latest engineering calculation procedures and dynamic simulation techniques and, when coupled with an engine control simulation, provided an excellent tool to investigate engine/control response. The control simulation was representative of a 1980's full-authority electronic control.*

*The rapid response schemes considered made use of engine variable geometry (airbleed, compressor stators, vanes, variable turbine areas and variable nozzle area) to match the engine to an approach configuration. The promising schemes were rematched to provide increased rotor speed and/or improved compressor surge margin. Rapid response was obtained during an acceleration from an aborted approach by rematching the engine back to the design configuration as the power lever was advanced to take-off.*



Noise levels of the rematched engine configurations were estimated, and the cost and weight penalties of incorporating the variable geometry schemes qualitatively assessed. Based on these studies it was determined that a modified version of the basic fuel control logic, together with a reset on the compressor stator vane schedule (both optimized for acceleration considerations), provided the best rapid response with negligible cost or weight increase. With this scheme the response time from approach (14.5 percent  $F_n$ ) to 95 percent take-off thrust was reduced from 2.85 seconds for the baseline acceleration to 1.3 seconds (current engines and controls perform the same transients in 4-5 seconds). The aircraft dynamics study indicates that this fast response is not necessary for an advanced technology CTOL transport; however, it may be important for short-haul, powered lift applications.

## INTRODUCTION

The engine cycle selected for an Advanced Technology Transport (ATT) aircraft planned for commercial operation in the 1980's considered low noise as one of the major design criteria. Additional reduction in the community noise exposure can be realized by adopting noise abatement procedures during take-off and landing. Specifically, the use of steeper approach glide slopes during the landing maneuver result in a significant reduction in the noise level. The reason for this noise reduction is twofold: (1) approaching at a steeper glide slope, the aircraft is higher at all points along the glide path, (2) less engine power is required to fly the aircraft at a steeper glide slope.

Before steeper glide slope approaches can be considered, studies must be made to assure that the present levels of air transport safety are not compromised. One major consideration is the engine thrust response necessary to assure positive climb gradients from an aborted landing with minimum altitude and speed loss. If the currently-required climb gradients are to be retained when utilizing increased glide slopes, it is possible that the response characteristics of the engine may have to be improved.

## AIRCRAFT DYNAMIC RESPONSE

It is expected that all future aircraft will have to meet present or lower FAA noise criteria. One of the methods capable of producing a significant reduction in noise during the approach phase of landing is the use of increased glide slopes. Since the thrust required during the approach condition and the altitude of the aircraft are directly related to the glide slope angle, the potential noise reduction results from both the lower thrust loading needed to maintain equilibrium and the increased altitude of the aircraft over the community.

The use of steeper approach angles, however, has the disadvantage of higher sink rates near the ground. An investigation of engine thrust response requirements was made with regard to an aborted landing and the transition from the higher glide slope angles to a conventional ( $3^\circ$ ) glide slope to determine what effect the increased sink rates had. A parametric variation of initial approach speed, maximum permissible angle of attack, glide slope angle, and one-engine-inoperative considerations was made.

The base point aircraft chosen for the evaluation was a three engine, Mach 0.90 design. The general aircraft characteristics are presented in Table I. The aircraft employed conventional control surfaces with an all moveable tail.

TABLE I  
GENERAL AIRCRAFT CHARACTERISTICS

Design Cruise Mach Number	0.90	
Sea Level Take-off Thrust	30,600 lbs/eng.	(136000 N)
Take-off Gross Weight	297,300 lbs	(134900 kg)
Maximum Landing Weight	252,700 lbs	(114600 kg)
Wing Loading	134 lb/ft <sup>2</sup>	(6416 N/m <sup>2</sup> )
Aspect Ratio	7.60	
Quarter Chord Sweep	36.5°	

The deflection rates and maximum deflection angles for the tail surfaces are presented in Table II.

TABLE II  
TAIL SURFACE DEFLECTION RATES AND MAXIMUM DEFLECTION ANGLES

Stabilizer Deflection

- Maximum Deflection +7°  
-5°
- Maximum Deflection Rate 1.2 deg/sec

Elevator Deflection

- Maximum Deflection +15°  
-25°
- Maximum Deflection Rate 25 deg./sec

In the analysis, the problem was assumed to be symmetric about a vertical plane through the longitudinal axis of the aircraft. With this assumption of lateral directional stability, the analysis reduced to three degrees of freedom: horizontal, vertical, and pitch. The problem was structured such that, for a specified glide slope and approach speed, the equilibrium conditions were determined. This steady-state condition yielded the approach power, angle of attack, and angular deflection of the tail surfaces needed to trim the aircraft in the approach phase. Table III presents the given and calculated information for the steady-state phase of the approach.

TABLE III  
STEADY-STATE APPROACH CONDITIONS

Flight Angle Velocity Altitude	}	Given Conditions
Surface Deflections Angle of Attack Approach Thrust	}	Calculated Output

As the aircraft, in a trimmed condition, passed through a given altitude, it was assumed that a decision was made to abort the landing and perform a missed approach. A delay of one second was assumed between the decision to initiate a missed approach and control actuation. This delay was thought to be a reasonable approximation of pilot reaction time. It was assumed that control column commands and thrust advance were performed simultaneously and were for a maximum performance maneuver. With the initiation of the missed approach maneuver, a time-dependent integration of the equations of motion was done to

calculate the resulting aircraft trajectory. These constraints are shown in Figure 1. The equations of motion referenced to a ground axis system are listed below, and the related force diagram is shown in Figure 2. In these equations the initial glide slope is considered negative.

### THREE DEGREES OF FREEDOM EQUATIONS OF MOTION

$$\Sigma F_{\text{HORIZONTAL}} = \text{THRUST} \times \cos(\alpha + \gamma) - \text{LIFT} \times \sin \gamma - \text{DRAG} \times \cos \gamma = \frac{W}{g} \frac{d}{dt} (V_{\text{HORIZONTAL}})$$

$$\Sigma F_{\text{VERTICAL}} = \text{THRUST} \times \sin(\alpha + \gamma) + \text{LIFT} \times \cos \gamma - \text{DRAG} \times \sin \gamma - W = \frac{W}{g} \frac{d}{dt} (V_{\text{VERTICAL}})$$

$$\Sigma M_{cg} = I_{zz} \times \frac{d^2 \phi}{dt^2}$$

$$\begin{aligned} \Sigma \text{MOMENTS} = & L_{\text{STAB}} \times \text{MOMENT ARM} + L_{\text{ELEV}} \times \text{MOMENT ARM} + \text{MAC} \\ & + \text{THRUST} \times \text{MOMENT ARM} \end{aligned}$$

$$L_{\text{STAB}} = \left( \frac{\partial C_L}{\partial \alpha} \right)_{\text{STAB}} \cdot \alpha_{\text{STAB}} \cdot S_{\text{STAB}} \cdot q \cdot l$$

$$L_{\text{ELEV}} = \left( \frac{\partial C_L}{\partial \delta} \right)_{\text{ELEV}} \cdot \delta_{\text{ELEV}} \cdot S_{\text{WING}} \cdot q \cdot l$$

$$\text{MAC} = C_{\text{MAC}} \cdot q \cdot S_w \cdot \bar{C}$$

$$\frac{d^2 \Phi}{dt^2} = \frac{\Sigma \text{MOMENTS}}{I_{zz}}$$

The thrust response of the engine was assumed to be a characteristic "S" shaped curve depicted in Figure 3. The response time of the engine was defined to be the time required to go from approach power to 95 percent take-off power. Under this assumption, response time becomes a function of approach glide slope. Determination of the time from idle power to 95 percent take-off power as a function of "response time" and glide slope is presented in Figure 4.

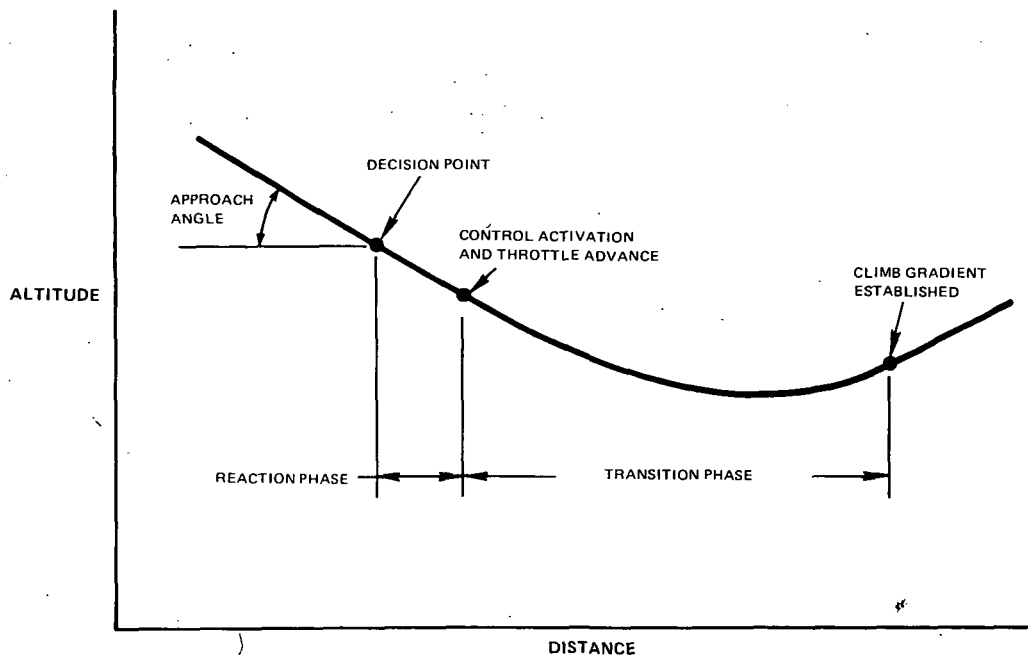


Figure 1 Approach Landing Go-Around

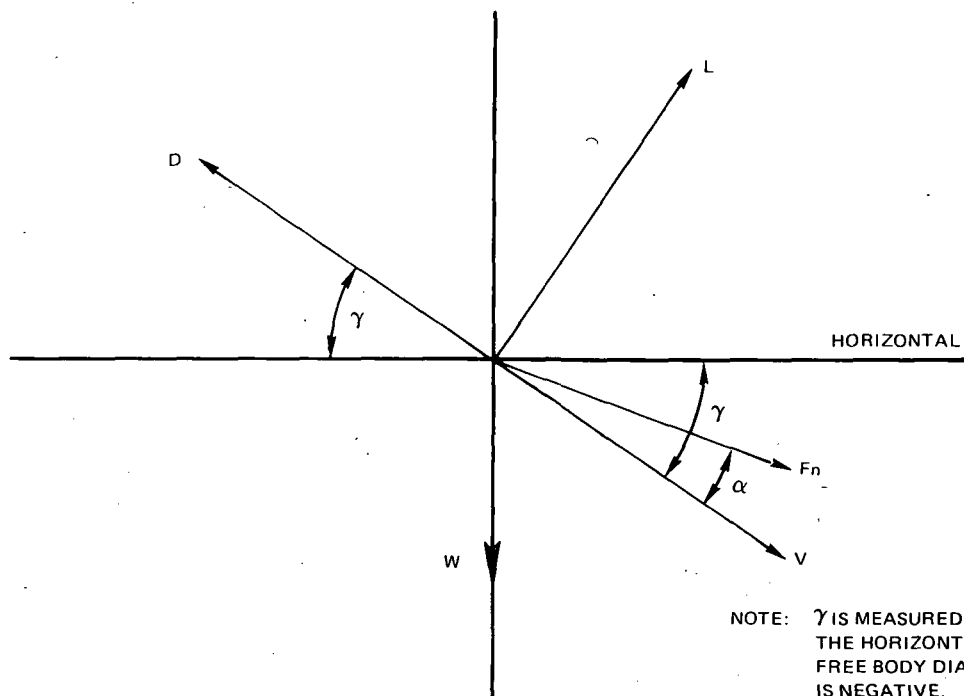
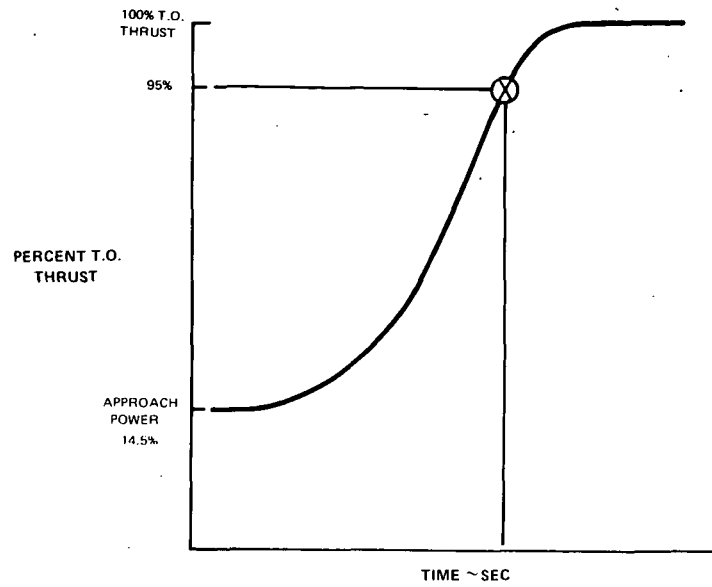


Figure 2 Free Body Diagram



RESPONSE TIME:  
TIME TO GO FROM APPROACH POWER TO 95% TAKE-OFF POWER

Figure 3 Thrust Response Characteristics

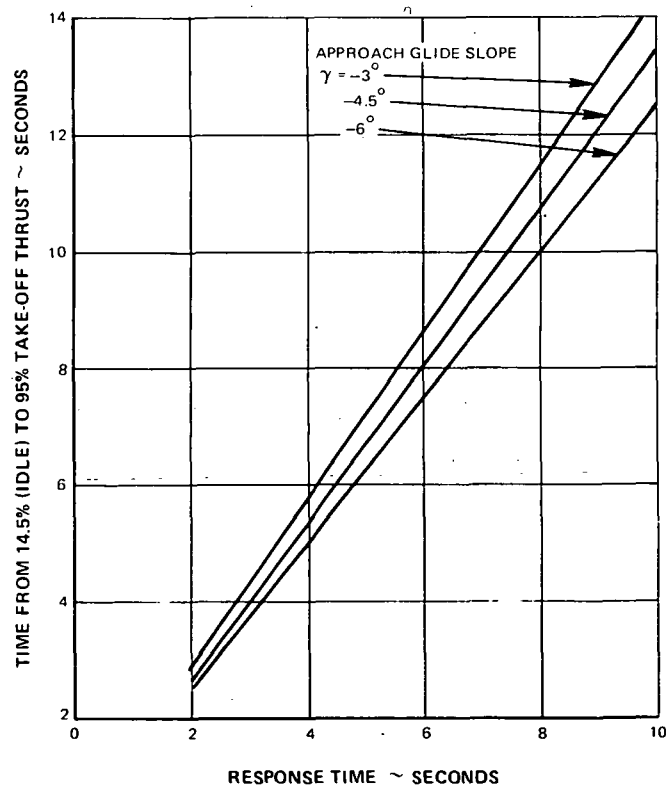


Figure 4 Engine Response Time

The angular acceleration or rotation rate of the aircraft was calculated assuming maximum surface deflection rates of the horizontal elevator and stabilizer. The aircraft was allowed to rotate from its steady-state angle of attack until an arbitrary limit on angle of attack was reached. Subsequently, the angle of attack was held constant. The limit on angle of attack was established to determine if the requirements for an adequate stall margin had a significant effect on the thrust response requirement. A consideration was also made of the effect of varying the aircraft response to control commands. This was attempted through a parametric variation of aircraft angular acceleration rates. The net effect of engine thrust response, aircraft rotation rate, and angle of attack limits determined the aircraft trajectory.

The aerodynamic characteristics of the aircraft are shown in Figure 5. Also shown are the steady-state angles of attack required to trim the aircraft for three different approach speeds. The ordinate is the body angle of attack. The wing is inclined  $2^\circ$  with respect to the body. Therefore, for example,  $15^\circ$  maximum angle of attack of the wing corresponds to  $13^\circ$  body angle of attack.

A series of aircraft trajectories is shown in Figure 6 for a  $6^\circ$  approach glide slope. As illustrated, the initial approach speed is 145 knots (74.6 m/sec) and the angle of attack of the wing is limited to  $15^\circ$ . These trajectory traces indicate that the response time of the engine does not seem to have a major impact on the total altitude loss in this type of maximum performance maneuver. In order to better define the requirements on engine response time, the following criteria were assumed:

- Upon the establishment of a positive climb gradient of 3.2% (approximately  $1.85^\circ$ ), the maneuver was considered terminated
- The positive climb gradient must be established within 8 seconds after the throttle advance
- The velocity at the end of the maneuver must be greater than, or equal to, the velocity at the initiation of the maneuver.

The points at which the 3.2 percent climb gradient is established are shown in Figure 6. It is apparent from the plot that, for the stated initial conditions, all the engines respond quickly enough to meet the requirement that the maneuver be completed within 8 seconds after the throttles have been advanced. It should be remembered that the elapsed time is measured from the decision point and that there is a 1 second delay after that point before the throttles are advanced.

The condition that the velocity at the end of the maneuver be greater than, or equal to, the velocity at the initiation of the maneuver is, however, not satisfied by all the engines. This is shown in Figure 7. This figure presents the velocity history for three approach speeds and four engine response times as a function of total elapsed time from the decision point in the maneuver. For each of the approach velocities, the steady-state trim conditions were determined separately - the lowest approach speed incurring the highest equilibrium angle of attack. Under the constraint of a  $15^\circ$  permissible maximum angle of attack, the 135 knots (69.5 m/sec)

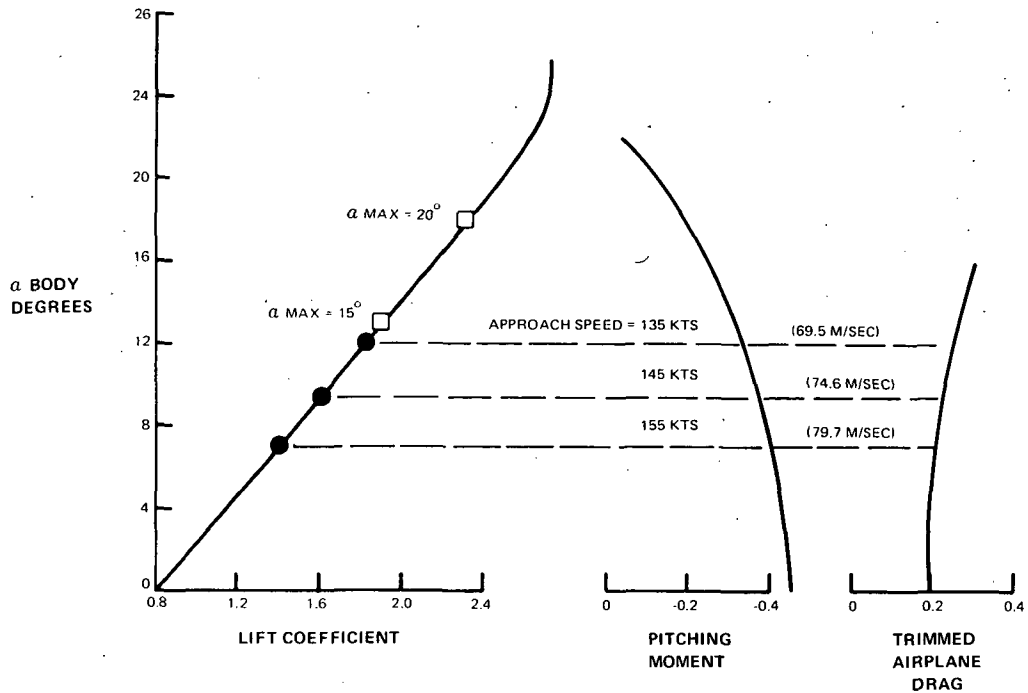


Figure 5 Low Speed Aerodynamics Characteristics

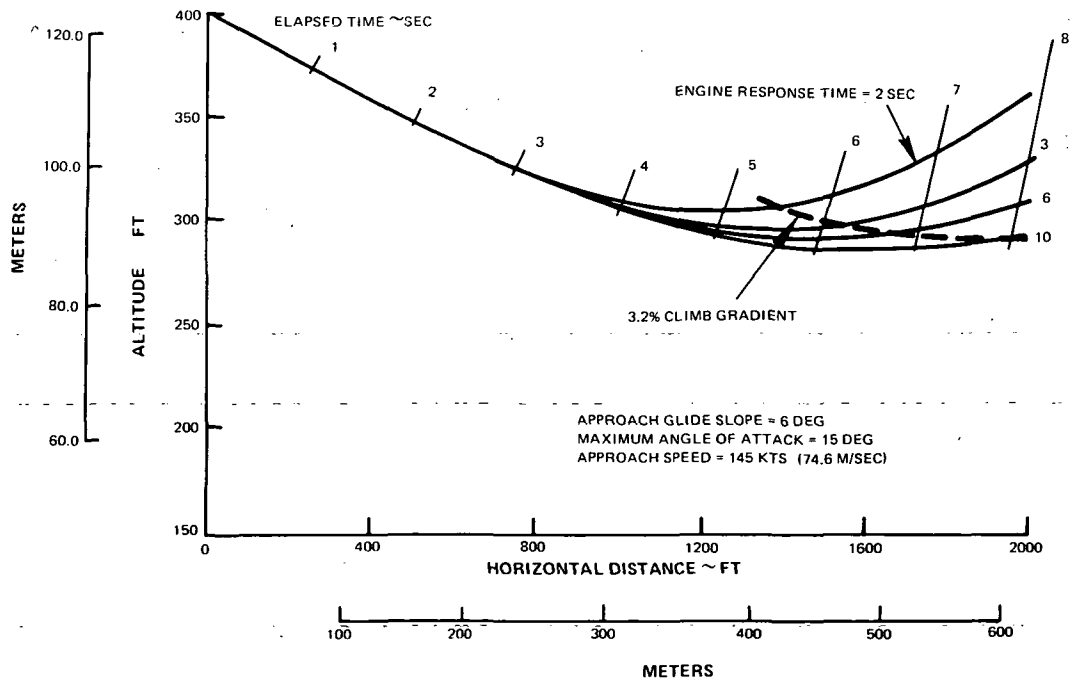


Figure 6 Effect of Engine Response Time on Flight Profile



approach speed case resulted in the smallest allowable angle of attack change, and thus the smallest change in drag coefficient. (This can be seen by referring to Figure 5.) Thus, essentially no velocity loss occurred anywhere in the maneuver. Increasing the approach speed does, however, result in a larger change in drag coefficient and thus a velocity loss is experienced for the slower responding engines.

The effect of increasing the maximum allowable angle of attack is demonstrated in Figures 8 and 9. It may be noted that the results for 20 and 25° maximum angle of attack differ only slightly. This is so because the aircraft is very close to the termination of the maneuver (establishment of a positive 3.2 percent climb gradient) by the time it has reached 20° angle of attack. Allowing the angle of attack to exceed 20° does not, therefore, result in a significant change in the result.

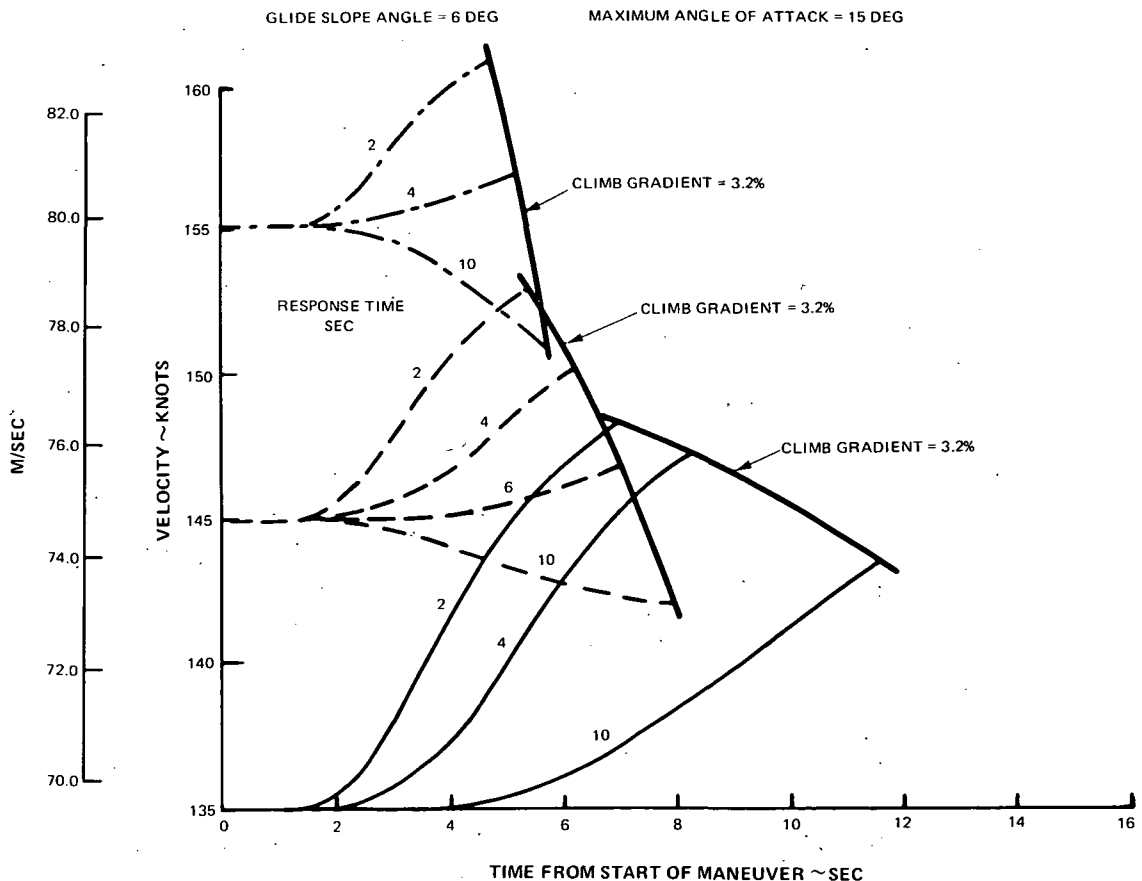


Figure 7 Effect of Engine Response Time and Approach Speed on Velocity History

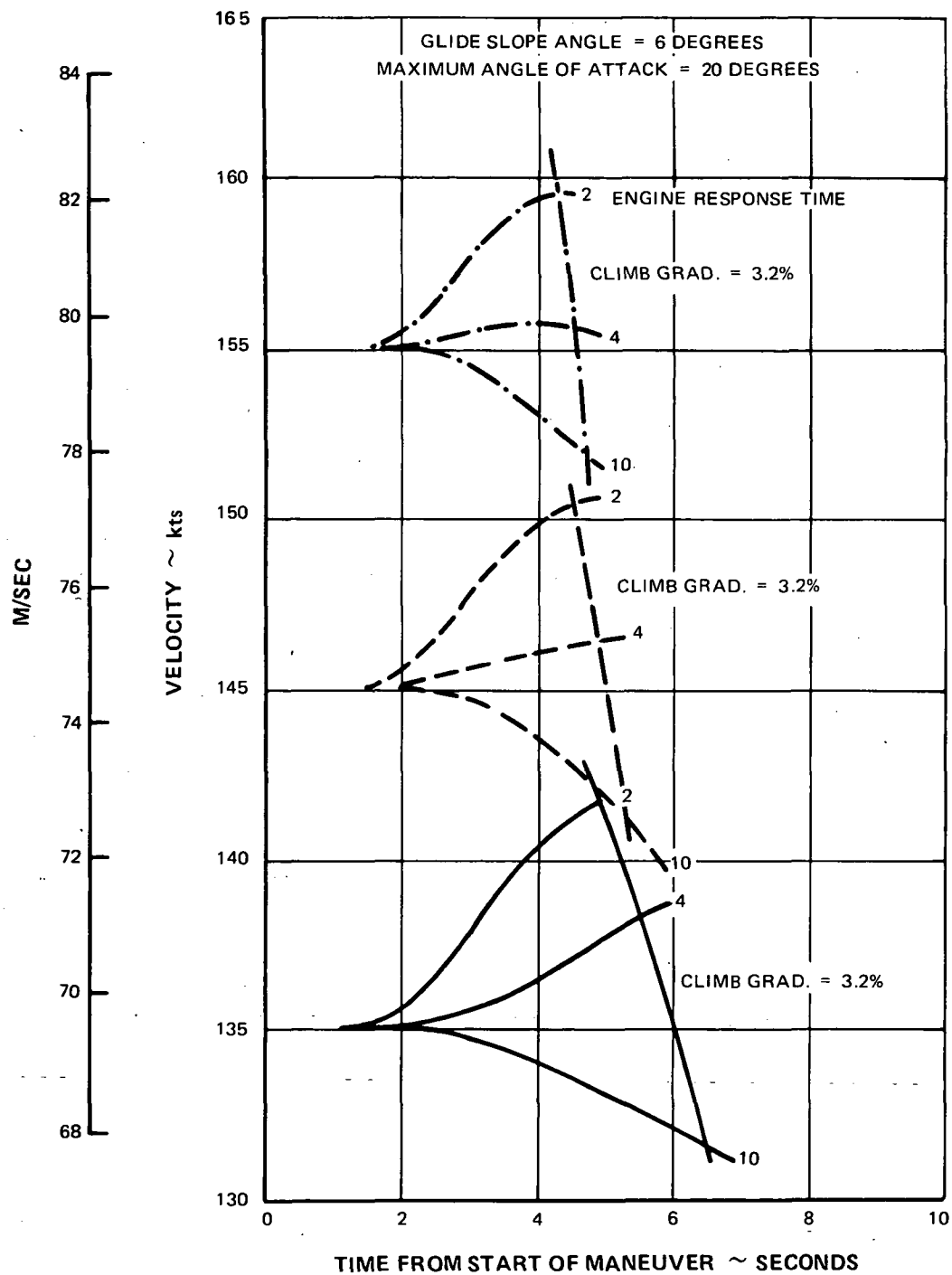


Figure 8 Effect of Engine Response Time and Approach Speed on Velocity History

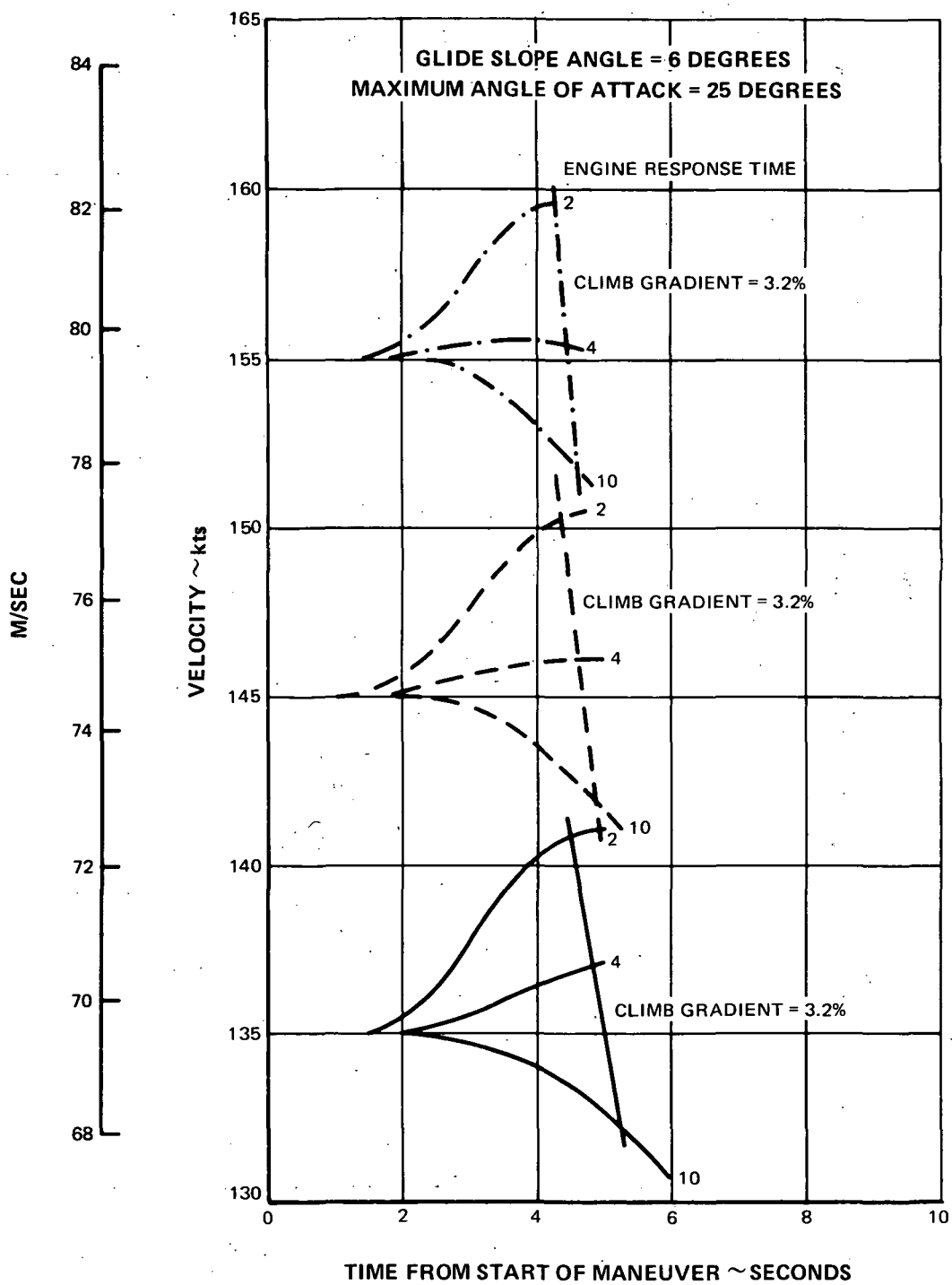


Figure 9 Effect of Engine Response Time and Approach Speed on Velocity History

A comparison of the velocity histories for a  $6^\circ$  and a conventional  $3^\circ$  approach is shown in Figure 10. The response time of the engine needed to satisfy the constraint of no velocity loss and an arbitrary gain of 3 knots (1.54 m/sec) in velocity is shown.

The major point of this figure is that the steeper ( $6^\circ$ ) glide slope permits a slower responding engine than the conventional ( $3^\circ$ ) glide slope. Since the maneuver was assumed terminated upon the establishment of a 3.2 percent climb gradient, the higher approach angle requires the velocity vector of the aircraft to be rotated through a larger angle. This is accomplished through the rotation of the aircraft itself. Since the engine thrust provides a relatively small contribution to the rotation rate of the aircraft, the rotation of the aircraft depends mainly on its response to control surface deflections. Therefore, since the time to complete the maneuver is smaller for the conventional approach, the engine must respond more quickly. Another factor that contributes to the slower response time requirement for the steeper approach is the fact that the component of aircraft weight in the direction of the flight path is approximately twice that for the conventional approach. This component tends to accelerate the aircraft. At any given time from the start of the maneuver the  $6^\circ$  approach angle has a greater increment in velocity than the  $3^\circ$  approach. This increment in velocity can be traded for engine response time. The forces acting during the maneuver are illustrated in Figures 11 and 12 for  $3^\circ$  and  $6^\circ$  glide slopes, respectively. The  $3^\circ$  and  $6^\circ$  missed approach maneuver are compared in Figure 13.

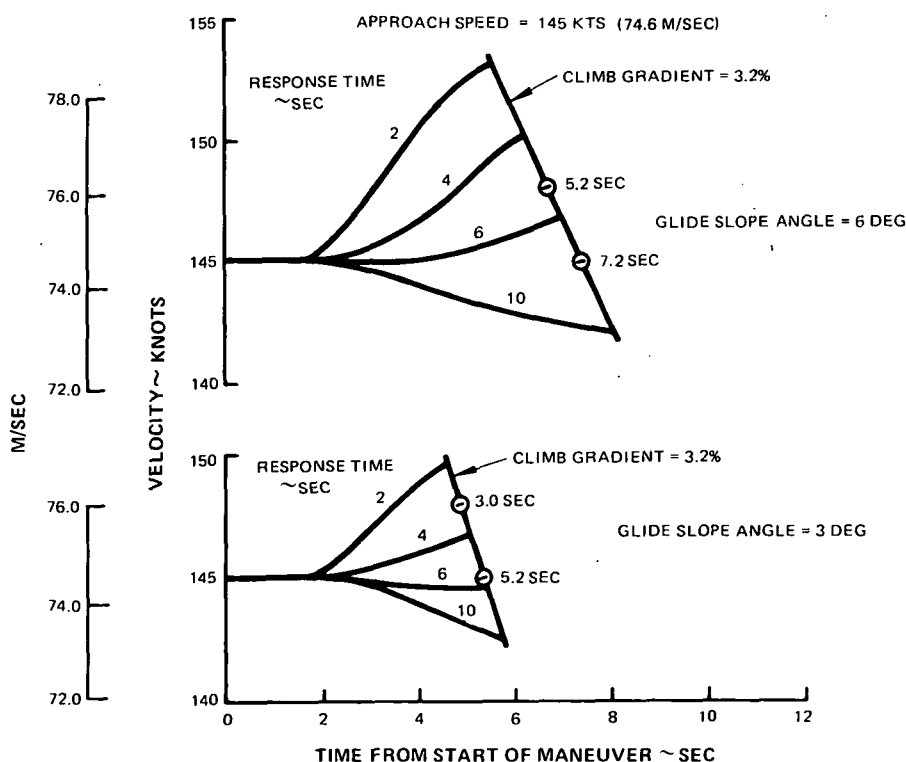


Figure 10 Effect of Glide Slope Angle on Velocity History and Required Response

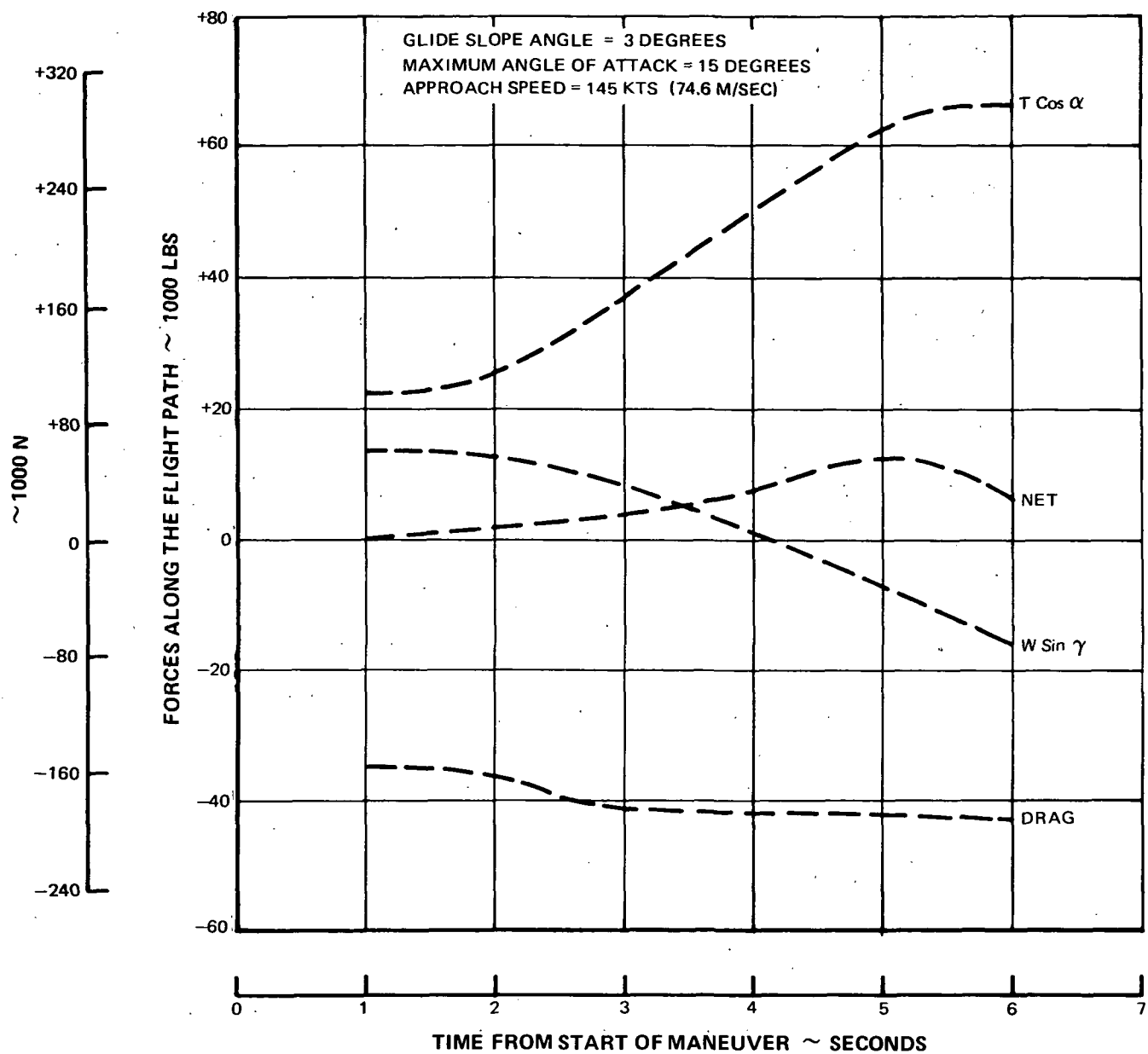


Figure 11 Component Forces Along the Flight Path

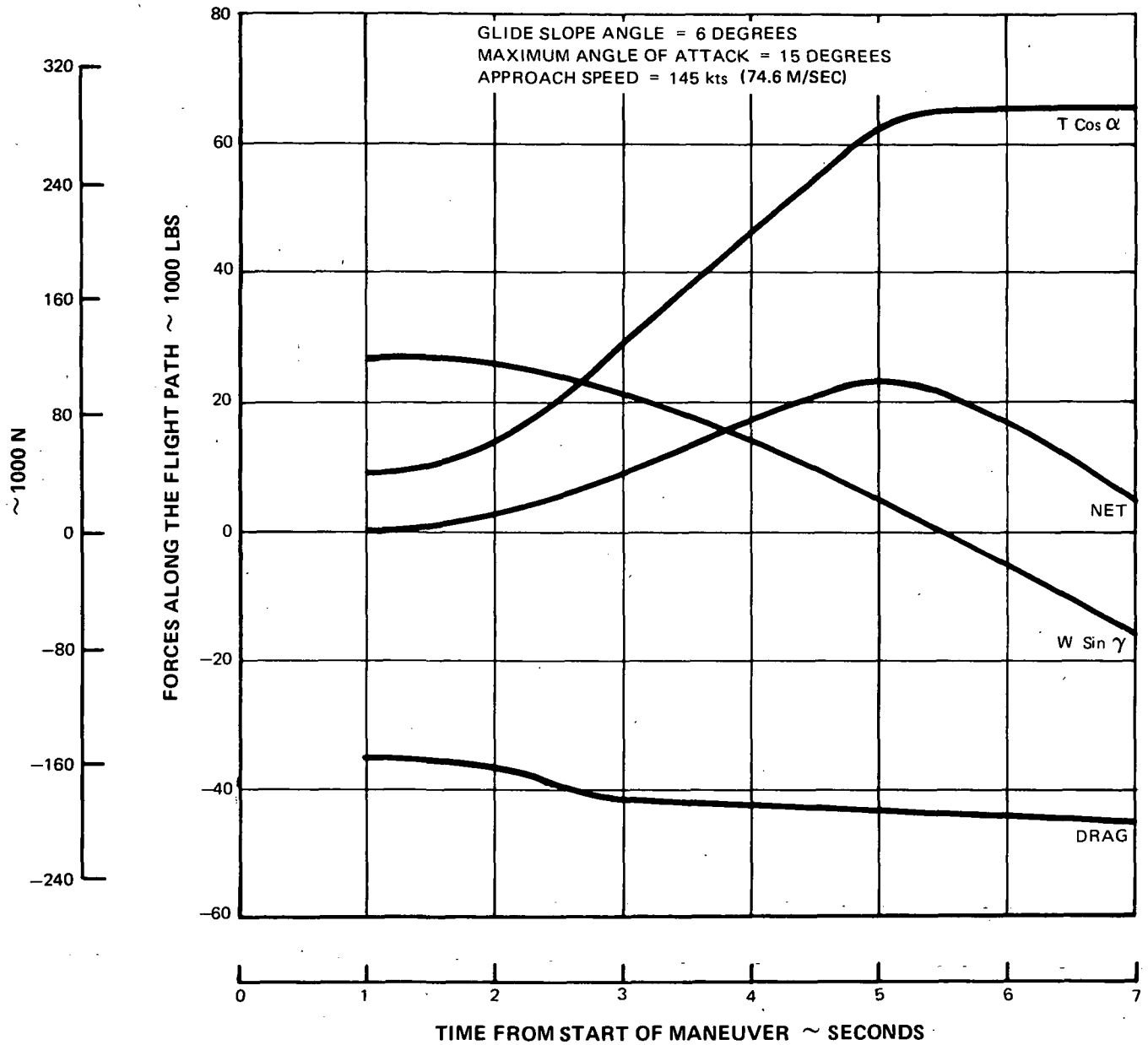


Figure 12 Component Forces Along the Flight Path

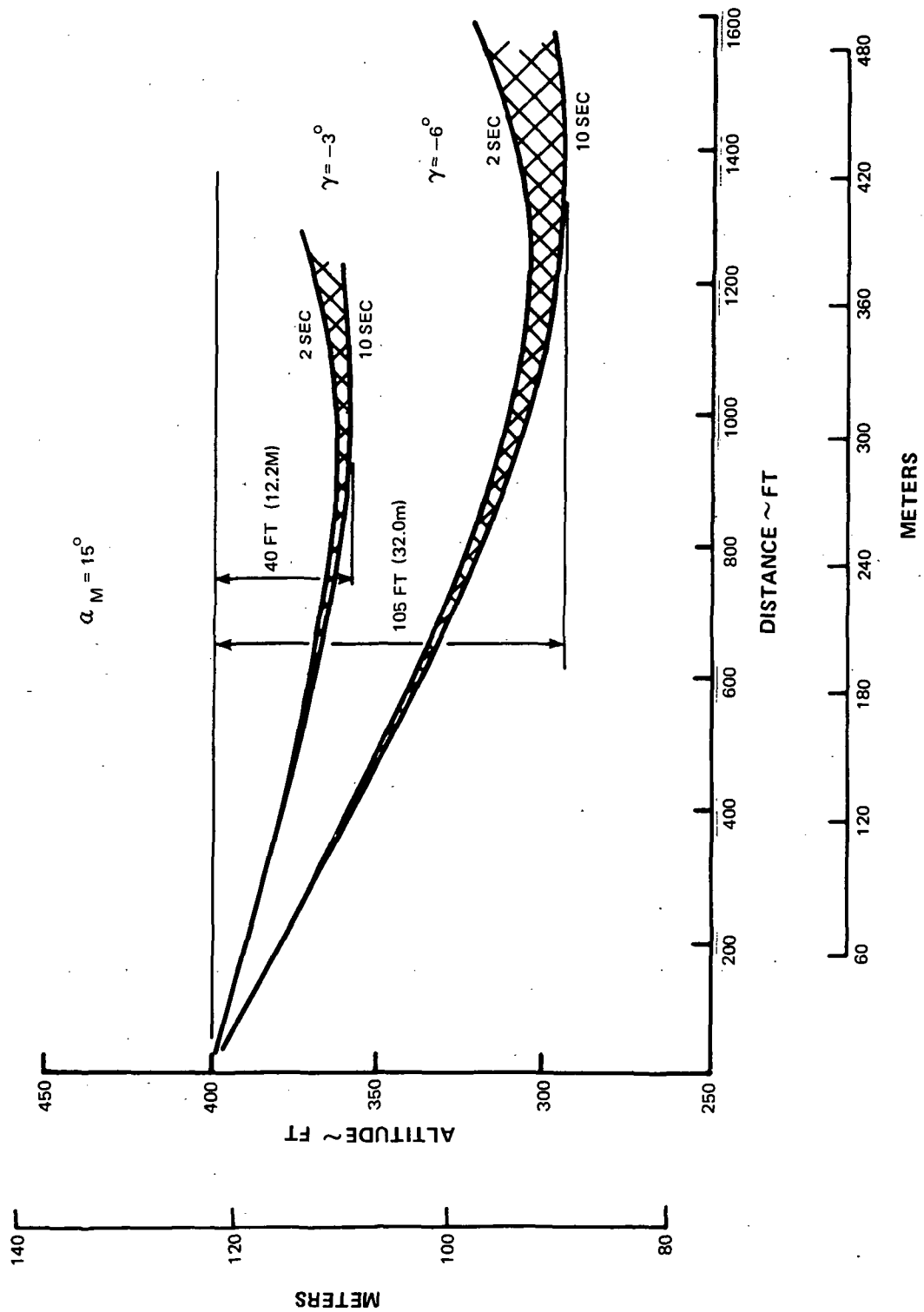


Figure 13 All Engines Operating

Whereas the steeper glide slope results in a less stringent requirement on engine response time, it does incur the larger altitude loss during the maneuver. The total altitude loss during the maneuver is shown in Figure 14. This case represents a limiting value of  $15^\circ$  on angle of attack. As was shown in Figure 7, the 135 knots (69.5 m/sec) approach speed is the least stringent in terms of required engine response but it suffers the greatest altitude loss. If the angle of attack is allowed to exceed  $15^\circ$ , the situation reverses and the 135 knots (69.5 m/sec) approach speed case results in the lowest altitude loss, as shown in Figure 15. This results from the fact that 135 knots (69.5 m/sec) case has the lowest initial sink rate.

In an effort to investigate the effect of an engine failure on the required response of an engine, it was assumed that the aircraft approached with all engines operating at the required approach thrust. Upon the failure of one engine, the remaining engines were brought up to full power and the aircraft rotation was initiated simultaneously.

Figure 16 demonstrates the results of this maneuver. Again it is seen that the steeper glide slope permits a slower responding engine. Even a "2 second" engine experiences some velocity loss early in the maneuver for the  $3^\circ$  approach case. The engine-out case requires a more responsive engine than that required by the all engines operating case, since the required thrust levels must be met by 2 rather than 3 engines.

The major conclusions of this study are summarized in Figure 17. As shown, if an arbitrary requirement of a three knot (1.54 m/sec) velocity increment at the end of the maneuver is postulated, the required response time of the engine is increased by approximately 2 seconds for all glide slope angles.

The use of increased glide slopes results in a less stringent requirement on engine response time. As stated previously, this results from the longer time required to turn the velocity vector of the aircraft. Thus, the required engine response becomes coupled to the aerodynamic capabilities of the aircraft and its ability to respond to control inputs.



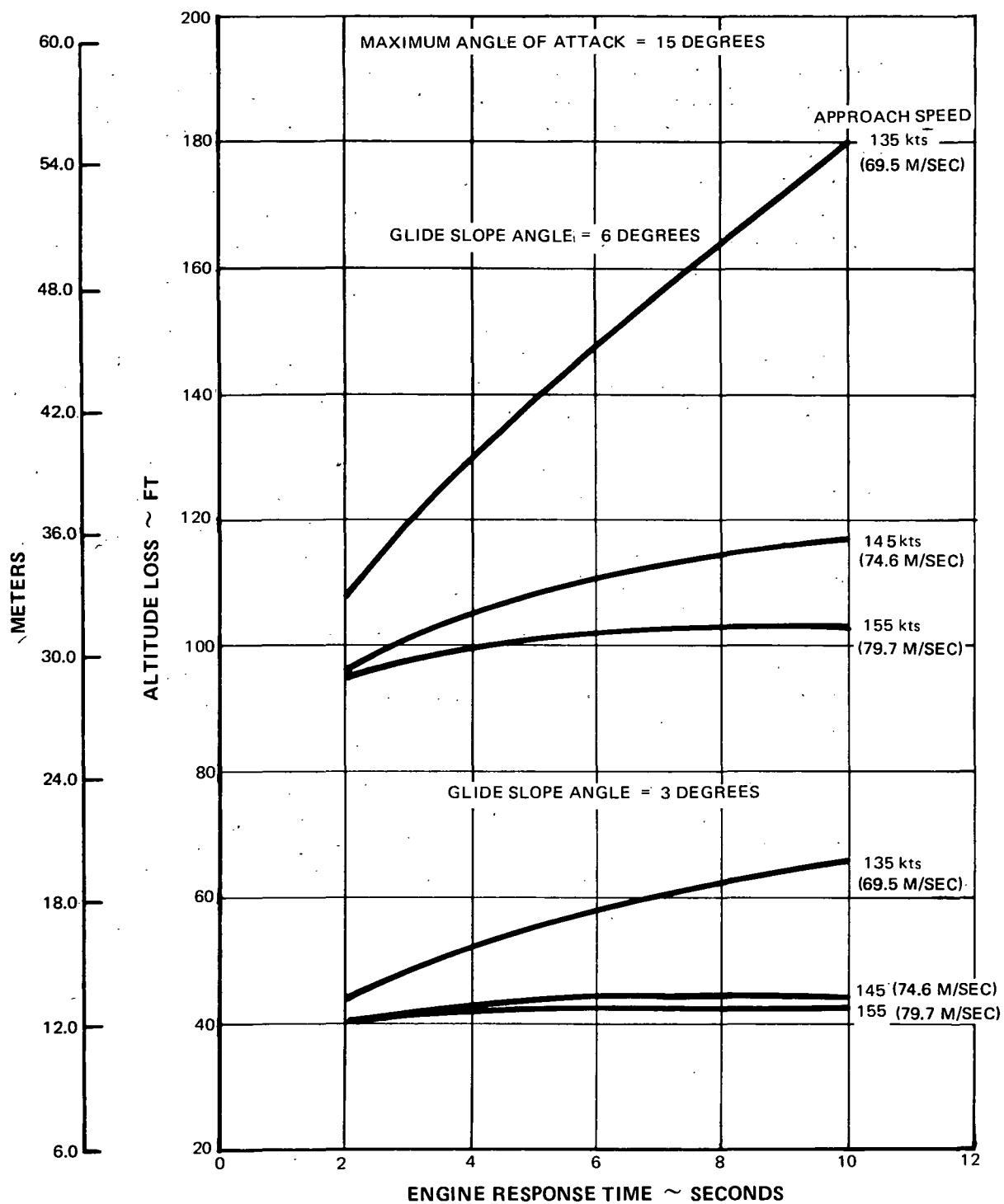


Figure 14 Total Altitude Loss

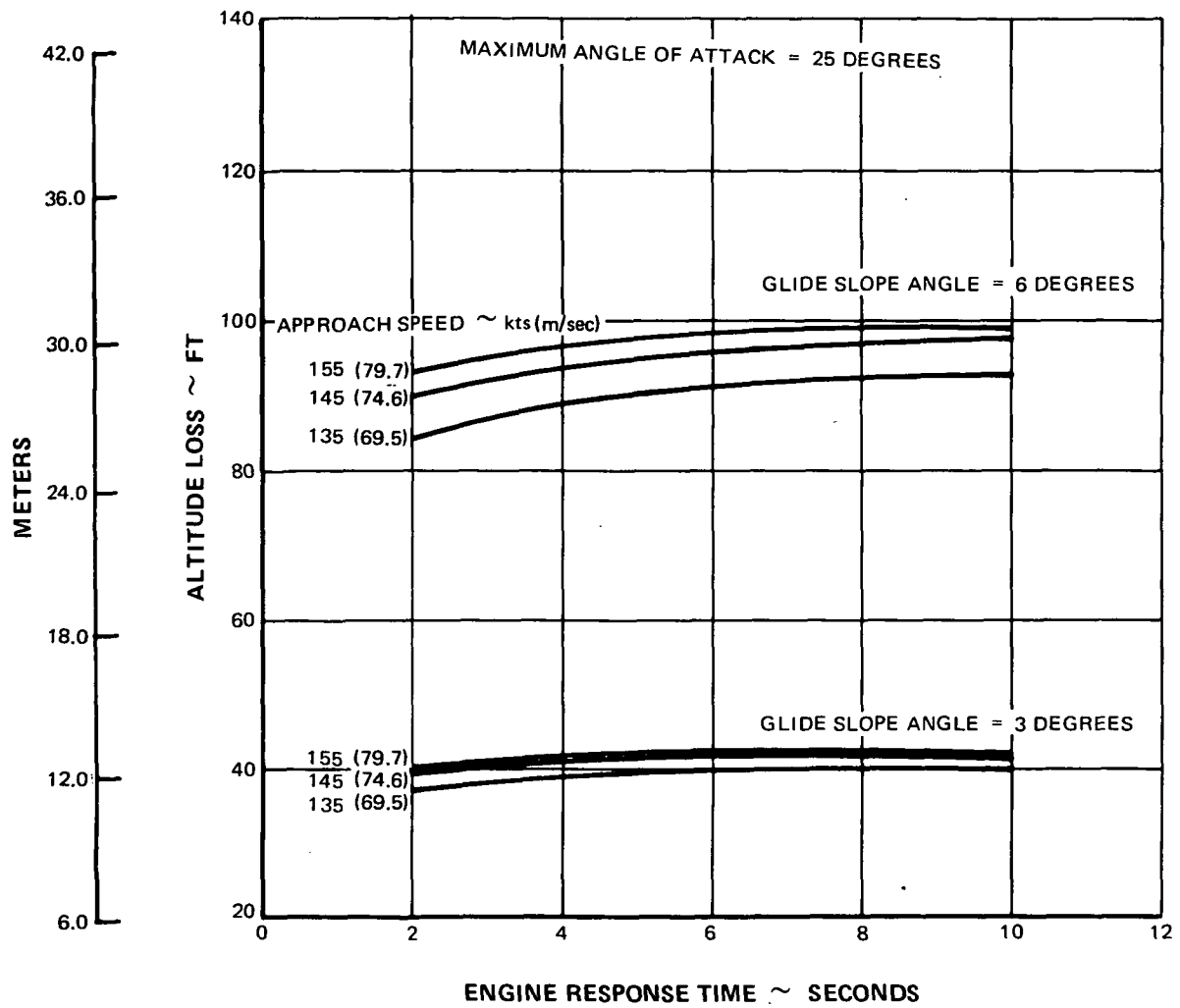


Figure 15 Total Altitude Loss

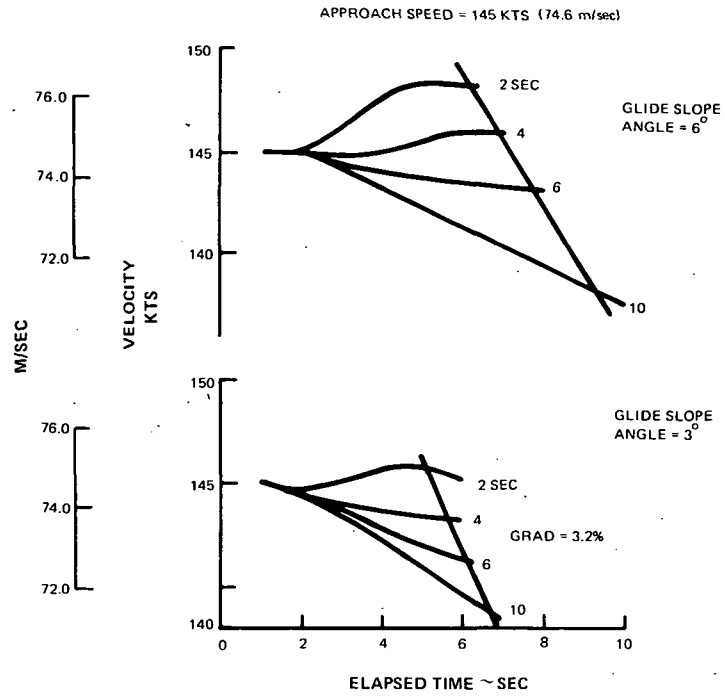


Figure 16 One Engine Inoperative

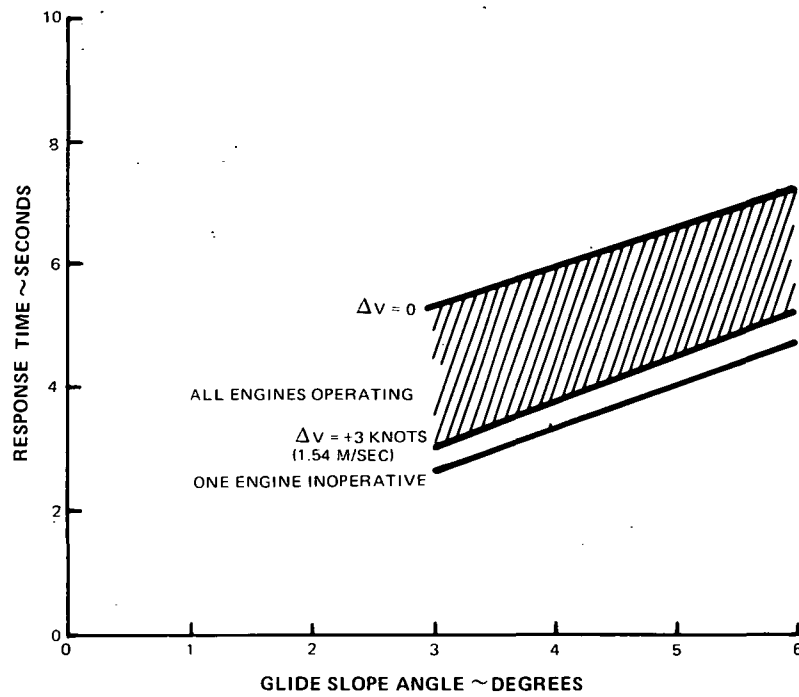


Figure 17 Summary of Engine Response Requirements ~ ATT Mach 0.9 Aircraft

## RAPID ENGINE RESPONSE

## BASIC CONTROL SYSTEM

Before studying rapid engine response schemes, it was necessary to first establish control system functions that would be representative of engine control technology in the 1980's, but relying on proven techniques wherever possible to minimize the study effort on this preliminary part of the program. The chosen design included variable compensation which would be implemented with a full authority electronic control. High rotor speed ( $N_2$ ) closed loop governing was selected as the primary control parameter with the reference speed scheduled from power lever angle and inlet total pressure and temperature. Additional loops provided low rotor ( $N_1$ ) overspeed protection and a combustor exit temperature (CET) limiter. A conventional fuel flow/burner pressure ( $W_f/P_b$ ) schedule limited the maximum fuel flow to provide adequate compressor surge margin and also limited the turbine over-temperature during accelerations. The deceleration fuel flow was also limited by a  $W_f/P_b$  schedule to prevent combustion instability.

Engine transfer functions were determined directly from the STF433 engine simulation using a state variable technique recently developed by P&WA<sup>TM</sup>. These functions were used to calculate the variable compensation necessary to assure good steady-state stability with fast transient response over the engine operating range from idle to take-off thrust. Figure 18 shows the engine response with this basic control system from idle to take-off thrust at sea level static, standard day conditions and from approach thrust to take-off at typical 6° approach conditions of 690 feet/155 knots (210m, 80m/sec), standard day + 18°F (+10°C).

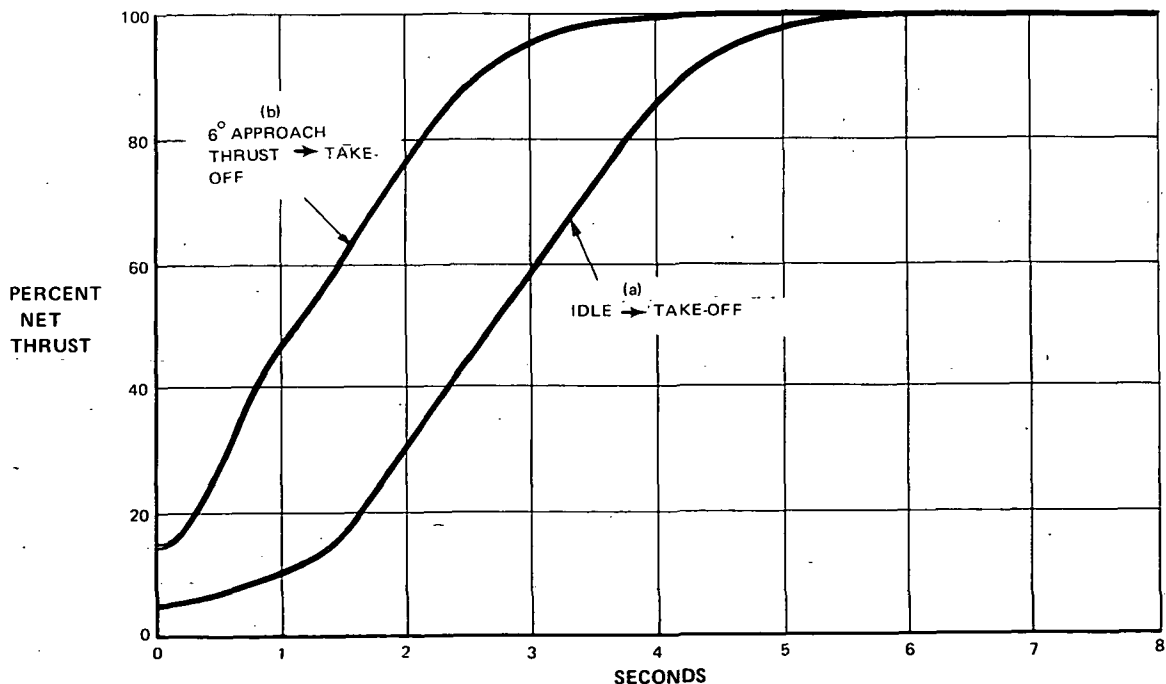


Figure 18. STF 433 Engine and Fuel Control Acceleration Characteristics ~ Basic Control

## RAPID RESPONSE SCHEMES – INTRODUCTION

It was demonstrated that improved approach to take-off thrust response can be achieved by:

- Matching the engine to an off-design configuration with variable geometry (air-bleed, nozzle area change, et cetera,) during the approach, then rematching to the design configuration at the decision to abort the landing. To maintain the approach thrust, the engine must operate at higher speeds. Thrust increases more rapidly than that of the baseline acceleration as a result of the efficiency increase during rematch and because the rotors accelerate from the higher speeds.
- Increasing the fuel energy input during the acceleration. This requires improved compressor surge margin which is obtained when the engine is rematched with variable geometry. Since the engine operates most efficiently at take-off thrust with the variable geometry in the design position (no airbleed, design stator vane angles, et cetera), this scheme also requires a different match during the approach. Transient rematch to the design configuration is performed during the acceleration.

The effects of off-design engine geometry on engine rematch at constant approach thrust were investigated to determine the changes in rotor speeds, compressor surge margin and combustor exit temperature. Only those configurations that rematched the engine to provide possible transient performance improvements were investigated further.

The effects of the following engine geometry variables were considered in the study:

- compressor bleed
- duct nozzle area
- overboard duct bleed
- primary nozzle area
- inlet airflow blockage
- compressor stator vane reset
- high pressure turbine area
- low pressure turbine area

In addition, modifications to the fuel control logic and the combined effects of this scheme with compressor stator vane reset and low pressure turbine variable geometry were also studied.

The rapid response schemes were evaluated for a  $6^\circ$  approach by comparison with the baseline response of 2.85 seconds from 14.5 to 95 percent take-off thrust as shown for  $6^\circ$  approach to take-off on curve (b) in Figure 18. Noise levels for the rematched approach configurations were compared with the baseline approach noise level of 71 ePNdB, for the  $6^\circ$  approach condition, estimated one nautical mile (1.852km) from the touchdown point (the noise level for a  $3^\circ$  approach at reduced height and increased thrust is estimated to be 88.3 ePNdB). The weight and cost penalties of each scheme were qualitatively determined.

### Compressor Bleed

The effects of compressor interstage and exit bleed on engine rematch at constant approach thrust are shown in Figure 19. The rotor speed increases would reduce the acceleration times with either scheme, but the higher combustor exit temperatures would limit the acceleration fuel flows. The increased surge margin would be advantageous only during the initial, non-temperature-limited part of the acceleration. After this point, the best acceleration would be obtained by gradually reducing the airbled fraction to provide the minimum surge margin with maximum allowable acceleration fuel flow. This scheme was demonstrated with compressor exit bleed and the acceleration time reduced by 0.15 second, not a significant saving considering the necessary control complication. From this evaluation, it was concluded that the use of compressor bleed is unattractive for fast thrust response.

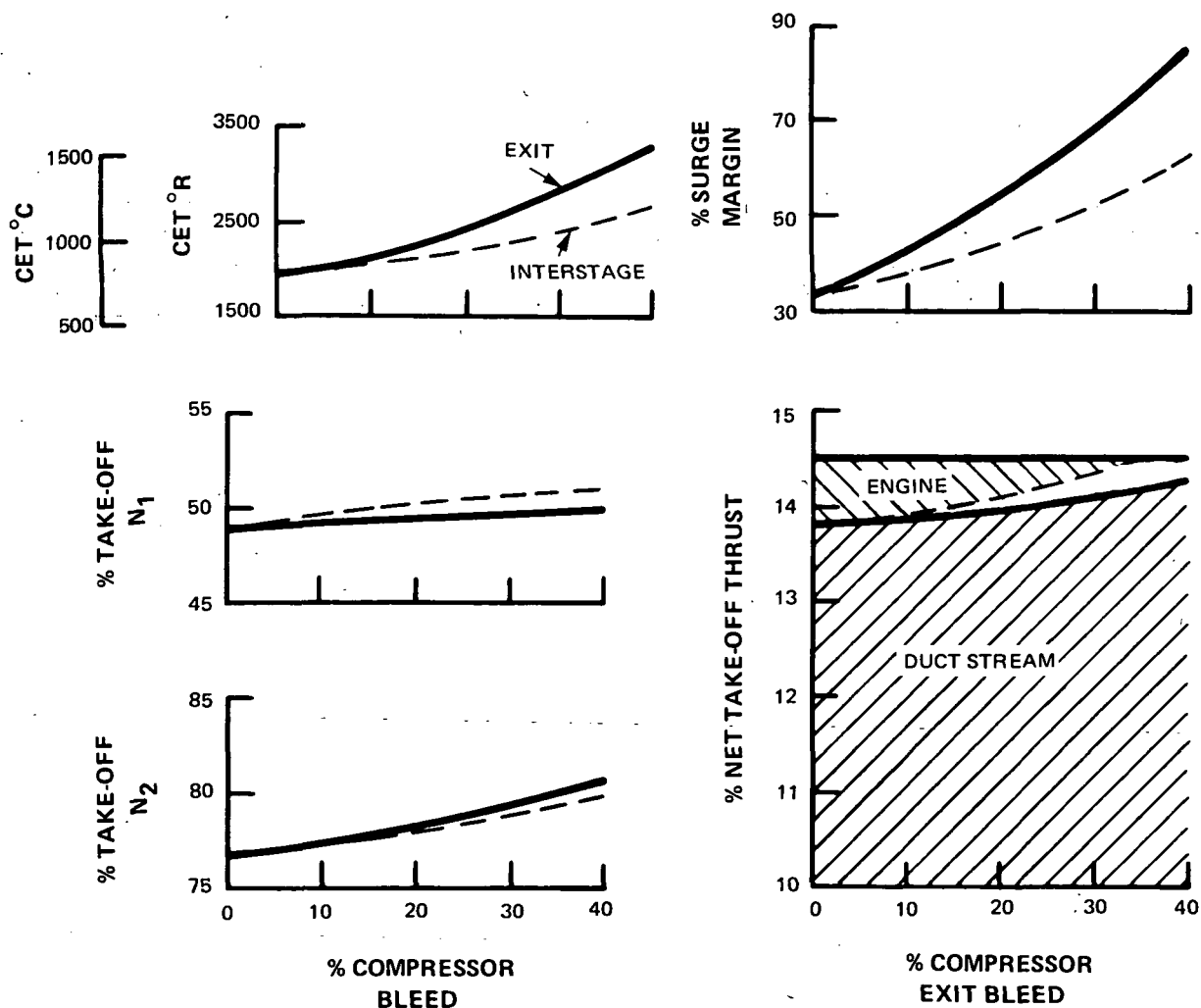


Figure 19 Steady-State Rematch with Compressor Bleeds ~ 6° Approach

### Duct Nozzle Variable Geometry

The effect of increased duct nozzle area ( $A_{jd}$ ) on engine match at constant approach thrust is shown in Figure 20. The increased rotor speed rematch with large areas is beneficial for fast response, as illustrated by Figure 21, which shows an acceleration from an approach configuration with a 100 percent nozzle area increase. In this transient, the nozzle area was reduced to the design value in one second, initiated at the time of power lever angle (PLA) movement.

The 2.4 second engine response time to 95 percent take-off thrust when rematched with 100 percent duct nozzle area increase is an improvement on the 2.85 second baseline acceleration time. However the increased cost and weight of the variable nozzle and the additional control functions does not justify the savings of 0.45 second. The 100 percent area increase would be difficult to achieve practically, and engine rematch with areas less than 100 percent increase would reduce the response time improvement.

The noise level of the rematched approach configuration measured one nautical mile (1.852 km) from the touchdown point was estimated to be 72.1 ePNdB.

An acceleration was also performed with a transient duct nozzle rematch. The nozzle area was transiently increased, then decreased to the design area during the acceleration. This would eliminate the high fuel consumption that results from the area reset on every approach. Figure 22 shows that the initial nozzle opening slows the thrust increase relative to the baseline acceleration and, although the thrust increases faster when the nozzle is closed, the overall effect is a longer acceleration time.

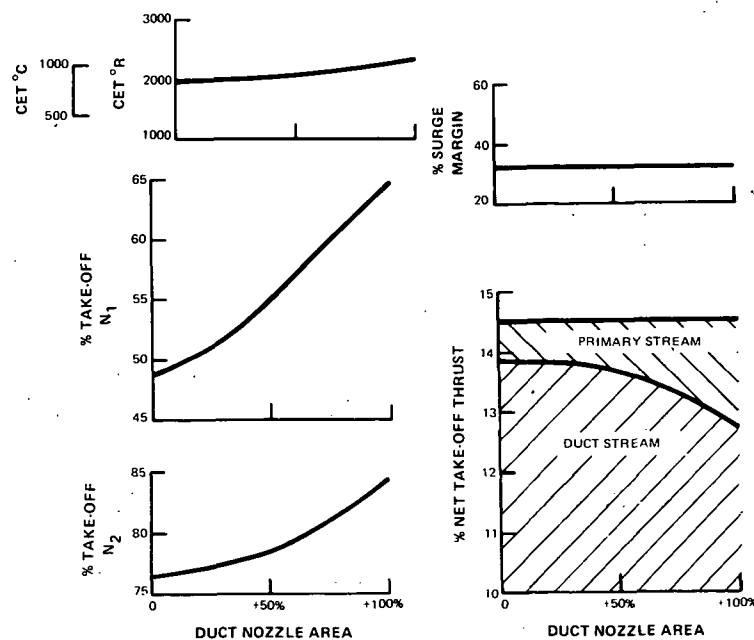


Figure 20 Steady-State Rematch with Variable Duct Area ( $A_{jd}$ )  $\sim 6^{\circ}$  Approach

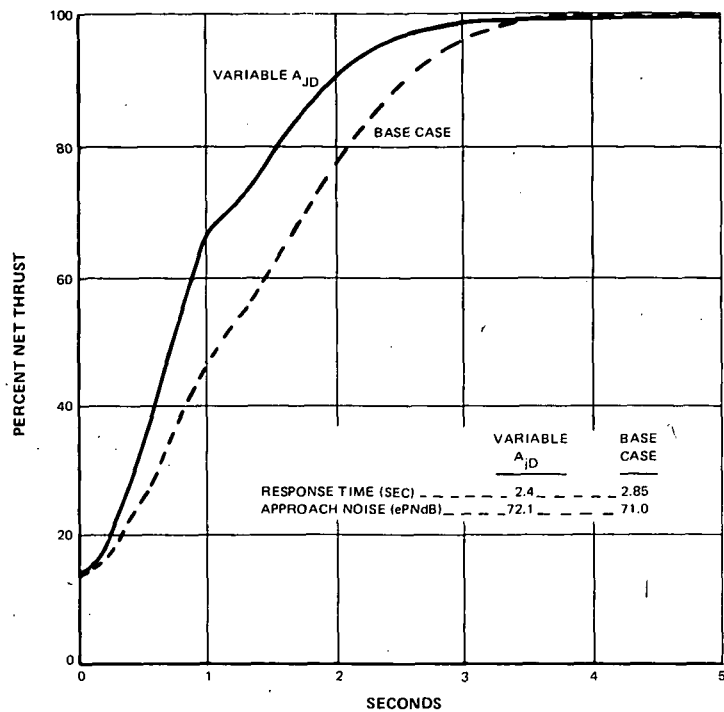


Figure 21 Variable Duct Area  $\sim 6^\circ$  Approach

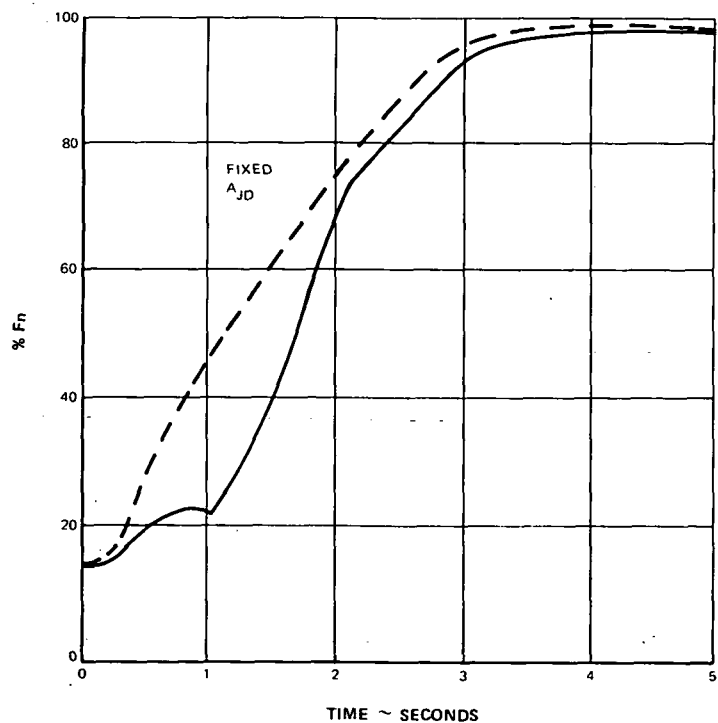


Figure 22 Transient Rematch with Variable Duct Area ( $A_{JD}$ )  $\sim 6^\circ$  Approach



### Overboard Duct Bleed

Overboard duct bleed rematches the engine in a similar manner to increased duct nozzle area with the exception that the sideways ejected air does not contribute thrust and the engine must operate at a higher level to maintain the approach thrust. The engine rematch necessary to maintain the approach thrust is shown in Figure 23.

The thrust response from an approach configuration rematched with 40 percent duct bleed is shown in Figure 24. Bleed was reduced at 100 percent-per-second, commencing from the initial PLA movement. The reduced bleed airflow alone provides a significant thrust increase with response proportional to the bleed valve closure rate. The response time of 1.25 seconds to 95 percent take-off thrust is a considerable reduction from the baseline acceleration time of 2.85 seconds; however, the increased approach noise level of 84.1 ePNdB due to the higher rotor speeds negates the environmental advantages of using of 6° glide slope approach. While a two-dimensional bleed valve system would be simpler than the duct three-dimensional variable nozzle of the previous scheme, the weight and cost penalties together with the increased noise make this scheme unattractive. The effect of the airbled on engine noise and the external flow characteristics around the engine nacelle were not considered in the evaluation.

### Primary Nozzle Variable Geometry

Figure 25 shows the engine rematch at constant approach thrust for increased and decreased primary nozzle area relative to the design value. The rotor speeds do not increase sufficiently with increased area to justify the complexity of a variable nozzle, consequently the scheme was not considered further.

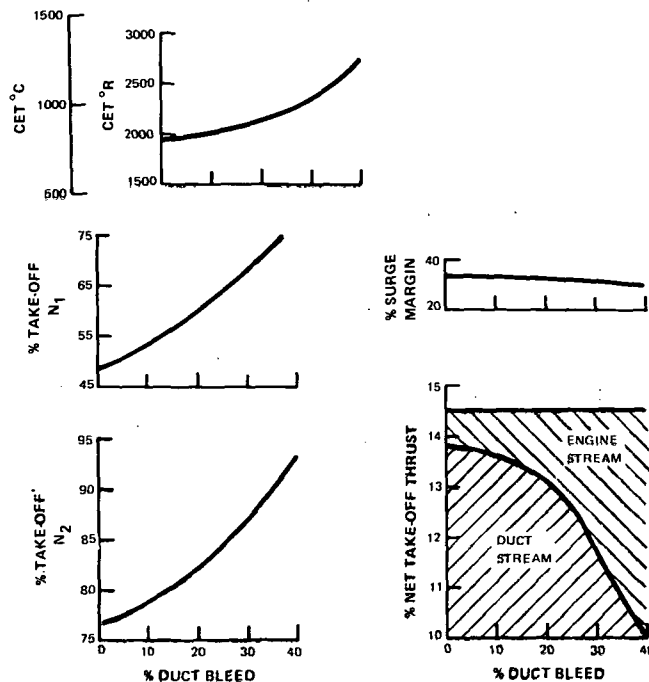


Figure 23 Steady-State Rematch with Duct Bleeds ~ 6° Approach

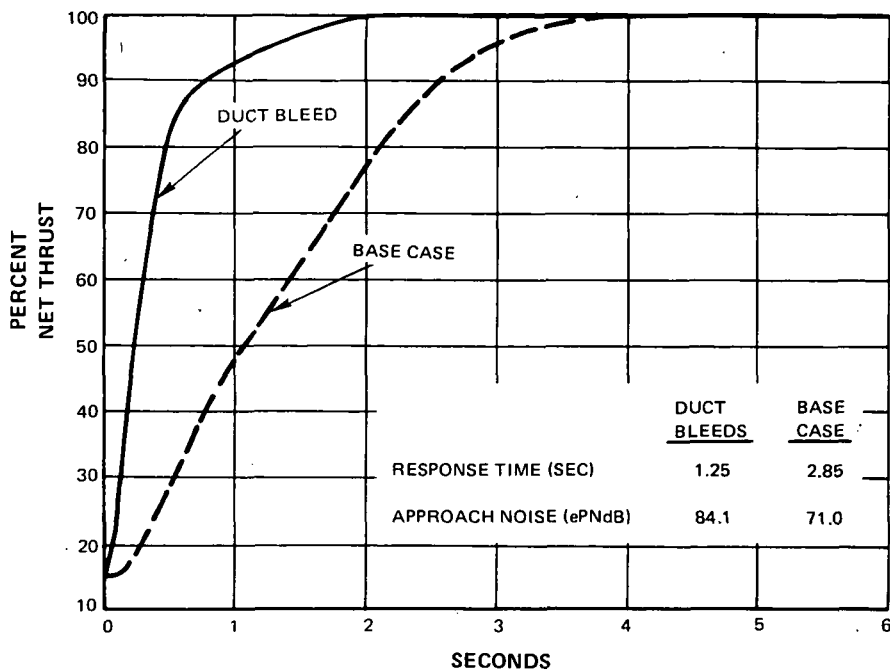


Figure 24 Steady-State Rematch with Duct Bleeds ~ 6° Approach

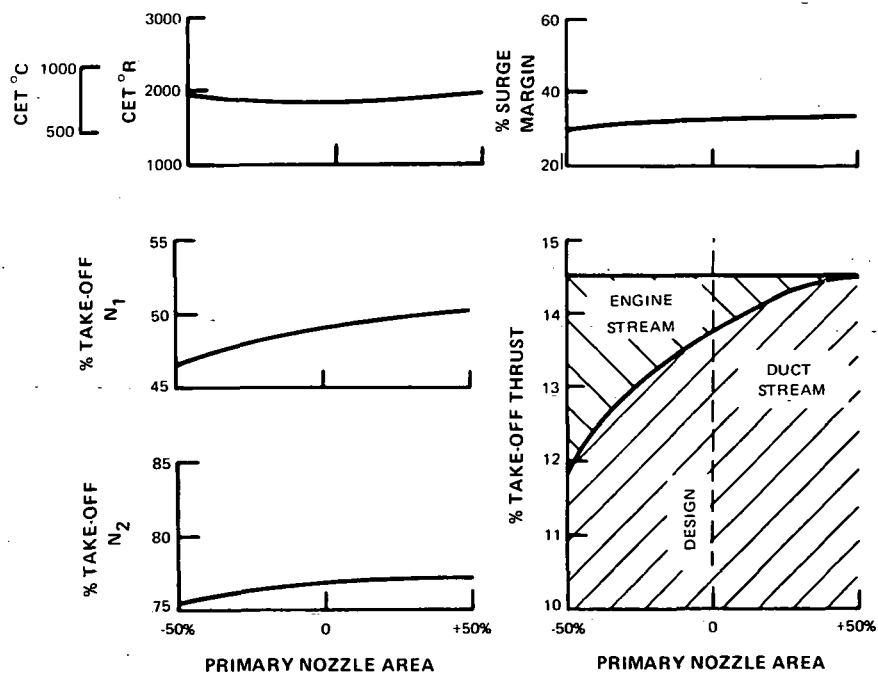


Figure 25 Steady-State Rematch with Engine Area ( $A_{JE}$ ) ~ 6° Approach

### Inlet Airflow Blockage

Inlet airflow blockers in the form of variable geometry retractable "fingers" reduces inlet efficiency and causes a reduction in engine inlet pressure, and an increased engine operating level is necessary to maintain the approach thrust. During a go-around acceleration the blockage would be removed to provide an immediate thrust increase and the rotors would accelerate to take-off faster because of the higher speed reset during approach.

The effect of reduced inlet pressure recovery on engine rematch at constant approach thrust is shown in Figure 26. This shows that pressure recoveries as low as 80-90 percent are required in order to rematch the rotor speeds to acceptable levels. Recent tests on choked inlet systems have shown that the airflow distortion resulting from inlet airflow blockage increases with decreased pressure recovery. The tests also indicate that the distortion associated with recoveries of 80-90 percent would be unacceptable. The scheme is also unattractive because the high noise levels (typically 88.7 ePNdB for a recovery of 83 percent), resulting from the increased jet velocity, negate the advantages of the 6° glide slope approach.

### Compressor Stator Vane Reset

The effects of compressor stator vane reset on engine rematch at constant approach thrust are shown in Figure 27. Compressor surge margin can be increased by closing the vanes without a significant increase in combustor exit temperature. For this reason, the scheme is more attractive than using compressor bleed.

In the acceleration shown in Figure 28, the stator vanes were slewed from a -10 degree approach reset to the scheduled position in one second, commencing from the PLA advance. The improved compressor surge margin obtained with the off-design stator angles allowed the acceleration schedule to be increased seven percent. The increased acceleration fuel flow and the higher rotor speeds during the approach both contribute to decreasing the acceleration time to 2.35 seconds. The 0.5 second improvement is significant, considering that this can be achieved by a minimum of modifications to an existing control function. The weight and cost penalties and the estimated noise level increase (71 to 71.5 ePNdB) for this scheme are considered to be negligible.

### High Pressure Turbine Variable Geometry

The effect of high pressure turbine variable geometry on engine rematch at constant approach thrust is shown in Figure 29. This indicates that, from a fast response consideration, the engine is probably best matched at the design area. Decreasing the area increases the high rotor speed but decreases the compressor surge margin, while improving the surge margin with increased area decreases the high rotor speed. The surge margin improvement obtained by increasing the area is also offset by the higher combustor exit temperature. As a result, this scheme was not considered further.

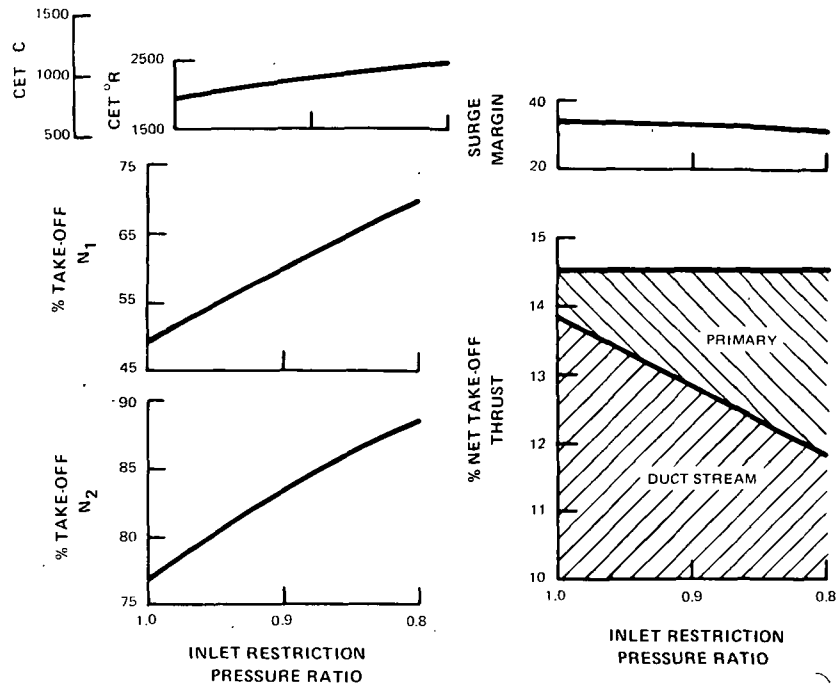


Figure 26 Steady-State Rematch with Flow Blockage in the Inlet ~ 6° Approach

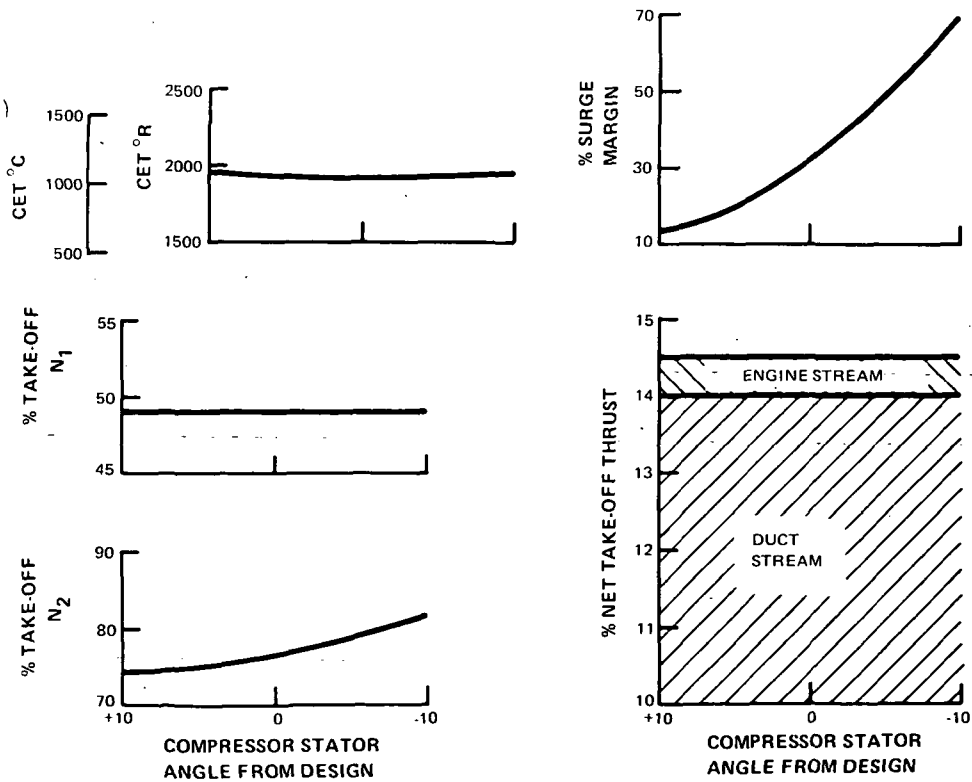


Figure 27 Steady-State Rematch with High Pressure Compressor Stator Vanes ~ 6° Approach

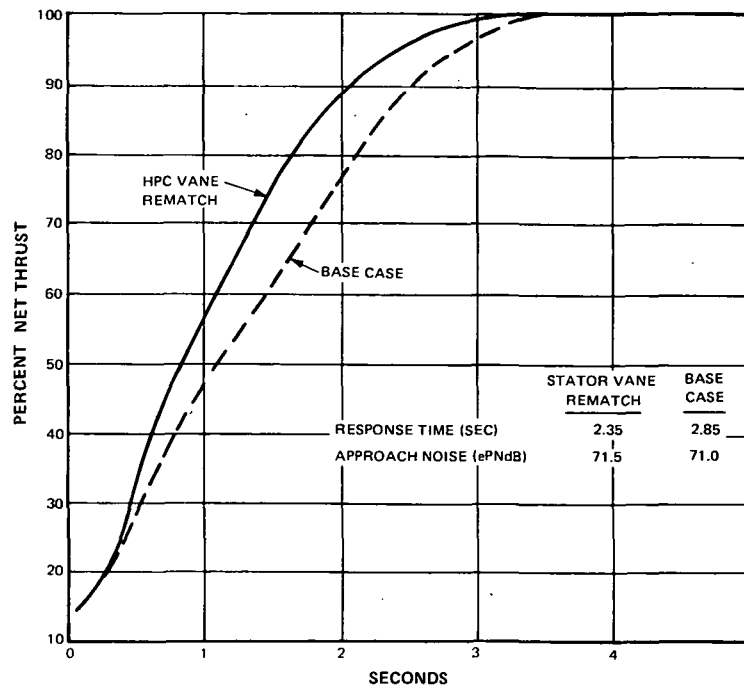


Figure 28 Compressor Stator Vane Rematch ~ 6° Approach

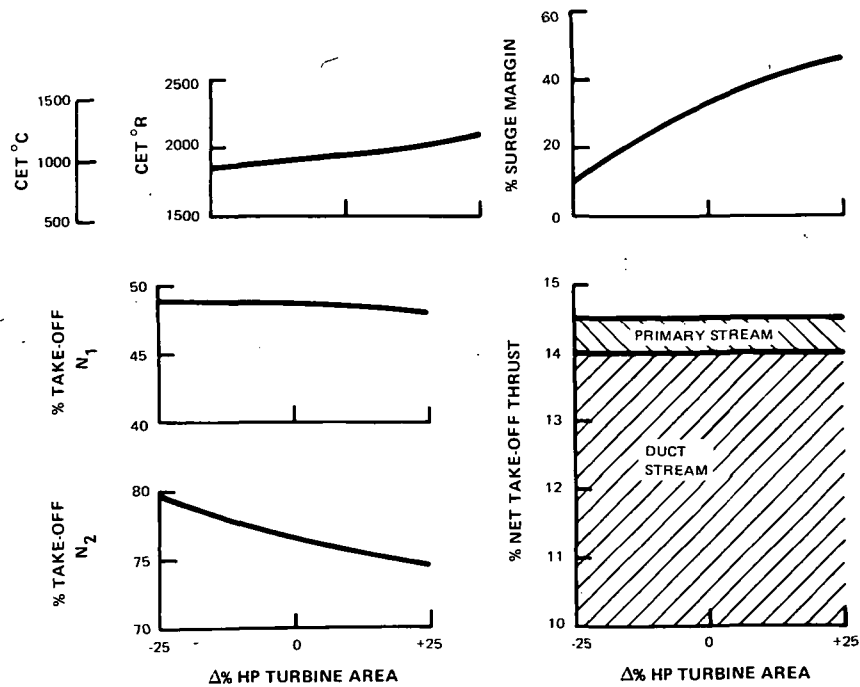


Figure 29 Steady-State Rematch with High Pressure Turbine Inlet Area ~ 6° Approach

### Low Pressure Turbine Variable Geometry

Figure 30 shows the effect of low pressure turbine variable geometry on engine rematch at constant approach thrust. Unlike the rematch with high pressure turbine variable geometry, it is now possible to increase the compressor surge margin and high rotor speed and decrease the combustor exit temperature, by increasing the low pressure turbine area.

An acceleration from the approach to take-off thrust, initially rematched with a 20 percent turbine area increase is shown in Figure 31. The increased compressor surge margin allowed the acceleration schedule to be increased seven percent. Low pressure turbine area was reduced to the design value in one second, commencing from the initial PLA movement. The decreased acceleration time is identical to the saving obtained with compressor stator vane reset, but weight and cost of a low pressure turbine variable geometry scheme would be too prohibitive to consider primarily for a rapid response scheme. However, if low pressure turbine variable geometry is required in the engine for other reasons, a rapid response scheme can be mechanized by adding another control function.

The noise level of the rematched approach configuration was estimated to be 71.3 ePNdB.

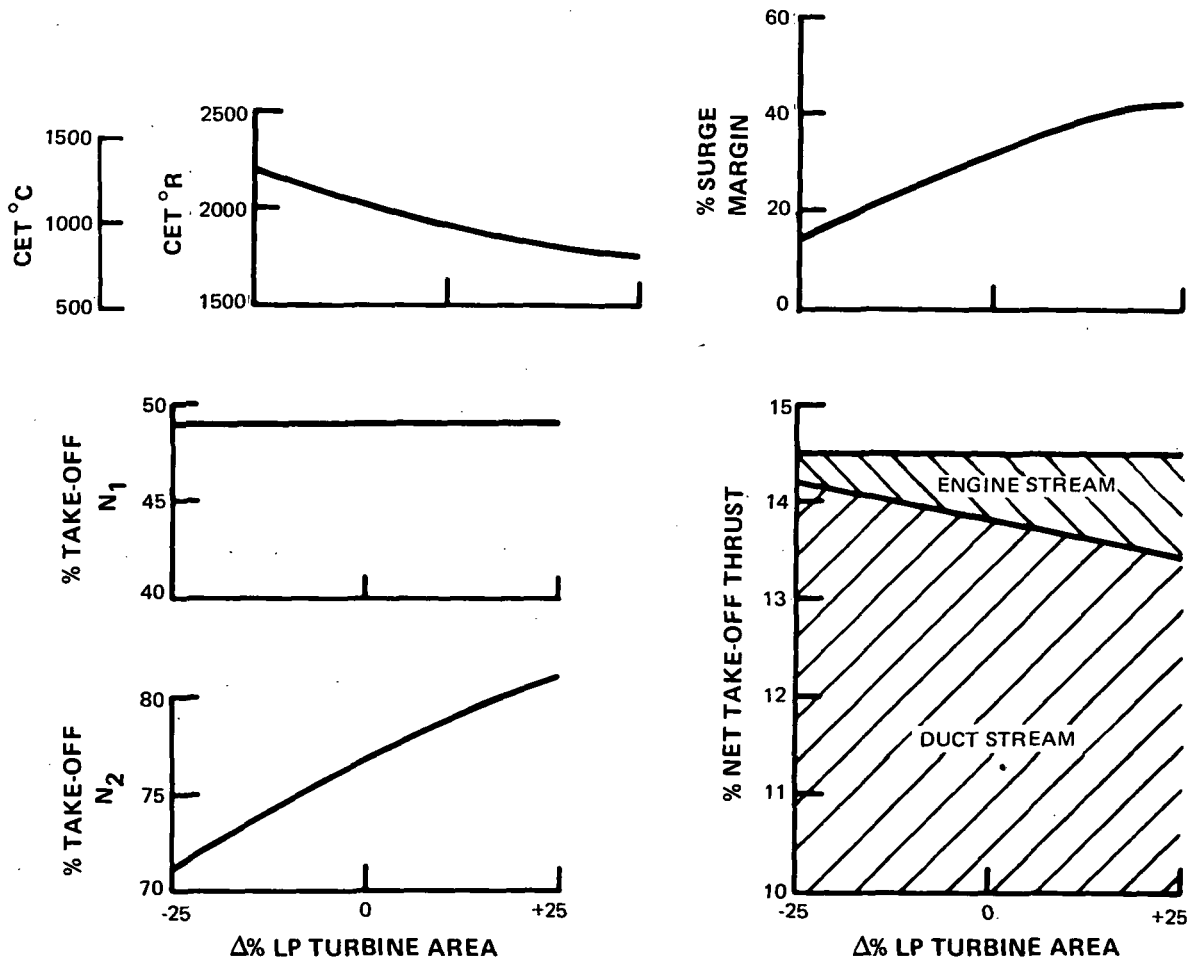


Figure 30 Steady-State Rematch with Low Pressure Turbine Inlet Area  $\sim 6^{\circ}$  Approach

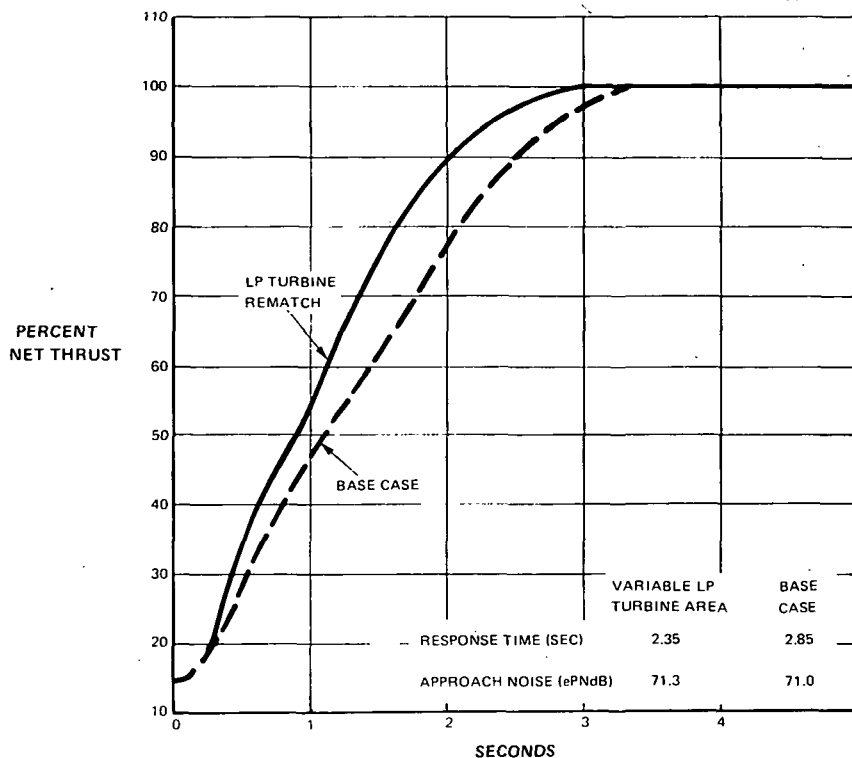


Figure 31 Low Pressure Turbine Area Rematch ~ 6° Approach

### Fuel Control Modifications

The fuel control incorporated variable lead/lag compensation to provide good steady-state stability and fast response for small perturbations; however, it demonstrated undesirable characteristics for large transients. During accelerations, for example, the high rotor speed lead compensation anticipated the final value and reduced the fuel flow from the acceleration schedule too soon, as shown on curve (a) in Figure 32. While this prolonged the acceleration, the transient performance of the basic control system was better than current transport engine-types which demonstrate similar characteristics.

The control logic was modified to improve the response by eliminating the compensation until the speed error approached zero. In Figure 32, the difference between the transient paths (a) and (b) indicates the additional fuel flow that can be added to the engine with the control modifications, without jeopardizing compressor surge margin or exceeding turbine temperature limits. Figure 33 shows the response improvements for sea-level/static, idle to take-off and 6° approach thrust to take-off transients, relative to the baseline engine/control performance. The acceleration time decrease from 2.85 seconds to 1.8 seconds at the approach condition represents a significant improvement in overall system performance. Since the faster response is obtainable with no change to the engine design, no increase in the approach noise and negligible increase in fuel control weight, size and cost, this is a most attractive scheme.

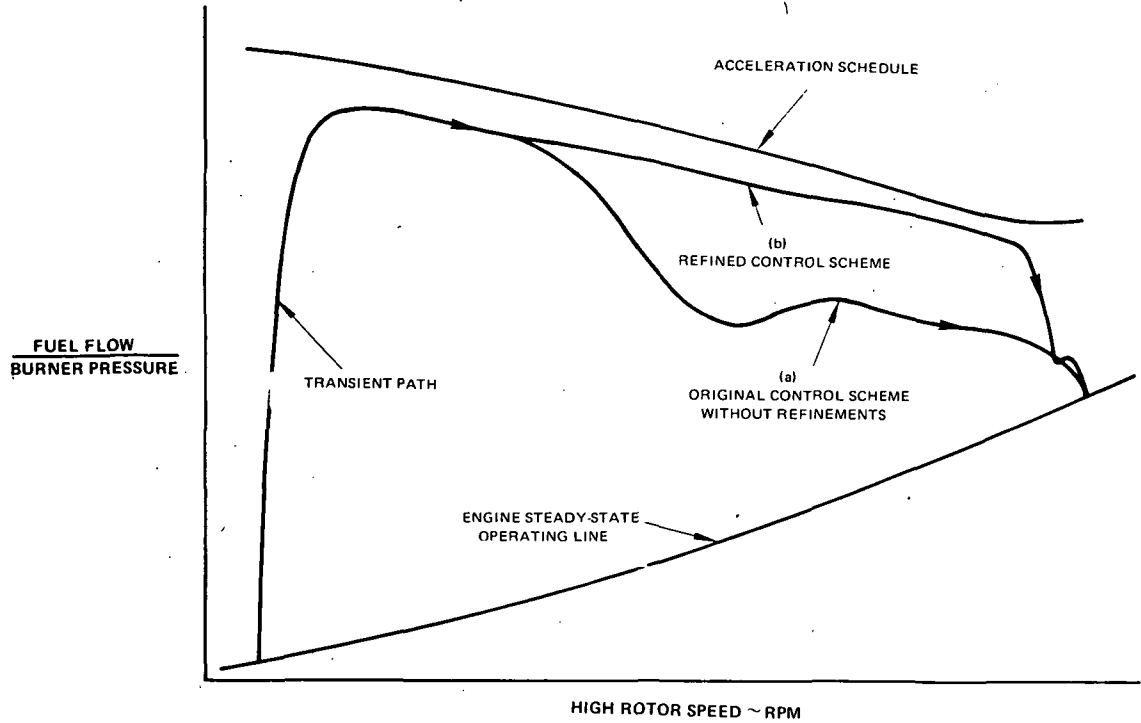


Figure 32 Modified Control Logic

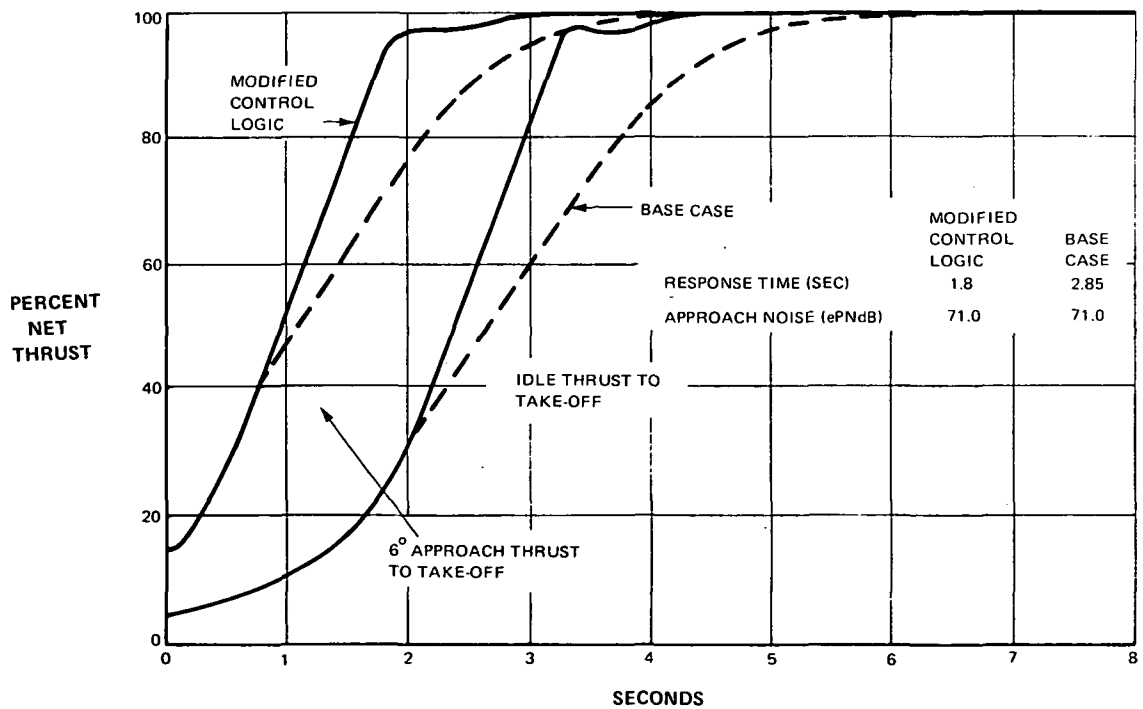


Figure 33 Modified Control Logic ~ 6° Approach



### Fuel Control Modifications With Compressor Stator Vane Reset and Low Pressure Turbine Variable Geometry

Performance of the modified control logic was demonstrated in combination with the compressor stator reset and low pressure turbine variable geometry schemes, Figures 34 and 35. The stator vane reset scheme provides an approach to 95 percent take-off thrust response of 1.3 seconds, and is preferred over the variable geometry turbine scheme because it has no impact on the engine design. To achieve the fast response, only the stator vane control would require an additional reset function since the fuel control modifications would be incorporated into the finalized design.

Finally, the modified control logic, compressor stator vane reset and low pressure turbine variable geometry schemes were combined. The acceleration shown in Figure 36 demonstrates an approach to 95 percent take-off thrust response time of one second with a fourteen percent increase on the base acceleration schedule. While this is an improvement on the response provided by the modified logic with the stator vane reset, the additional weight and cost penalties of the variable geometry turbine cannot be justified in this instance, although for other applications (V/STOL for example) the scheme may be worthwhile.

A summary of the promising schemes investigated in the study is shown in Figure 37. Various methods were used to reduce acceleration time from the base case of 2.85 seconds to 1.0 second on approach transients from 15 to 95 percent thrust. With the exception of the duct bleed scheme, the approach noise for the various schemes remained relatively constant at the base case level.

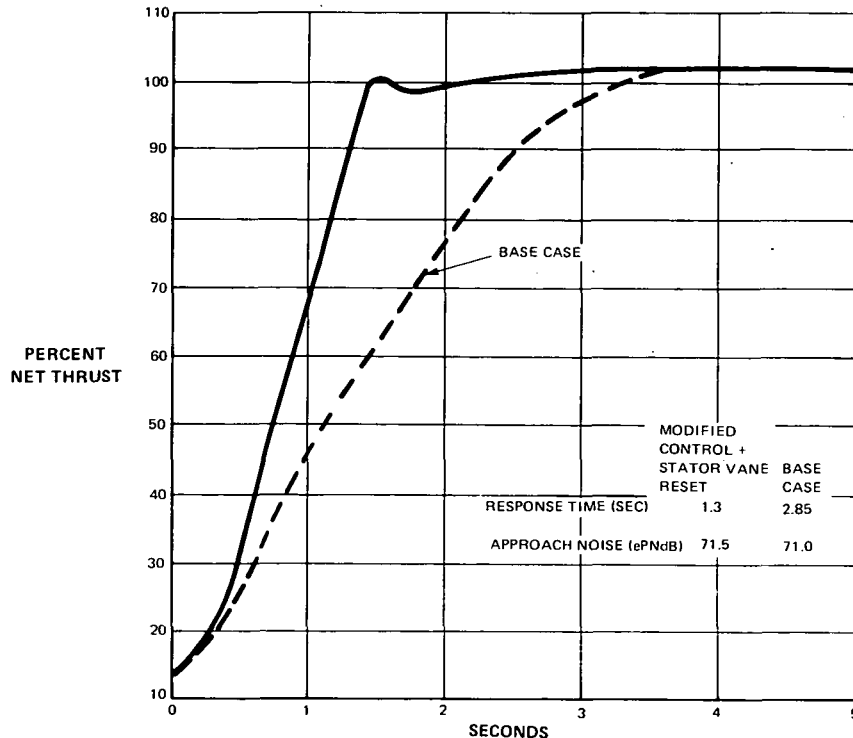


Figure 34 Combining Modified Control Logic and Stator Vane Reset ~ 6° Approach

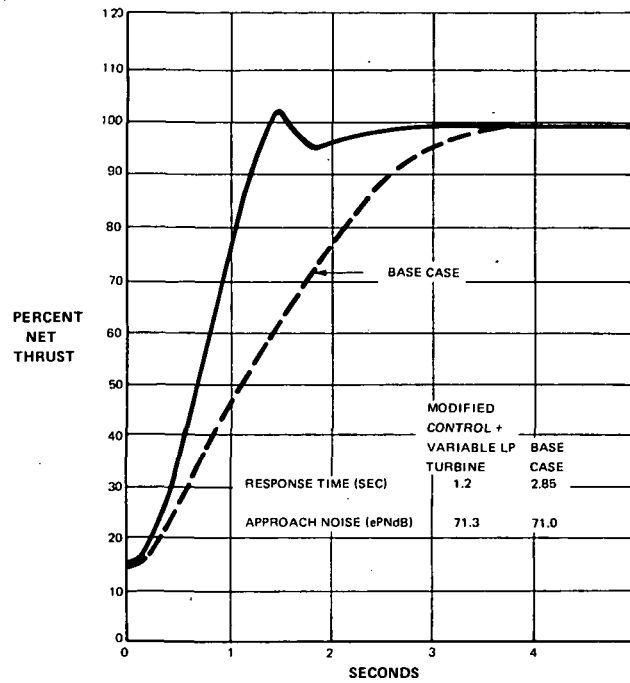


Figure 35 Combining Modified Control Logic and Variable Low Pressure Turbine Area  $\sim 6^\circ$  Approach

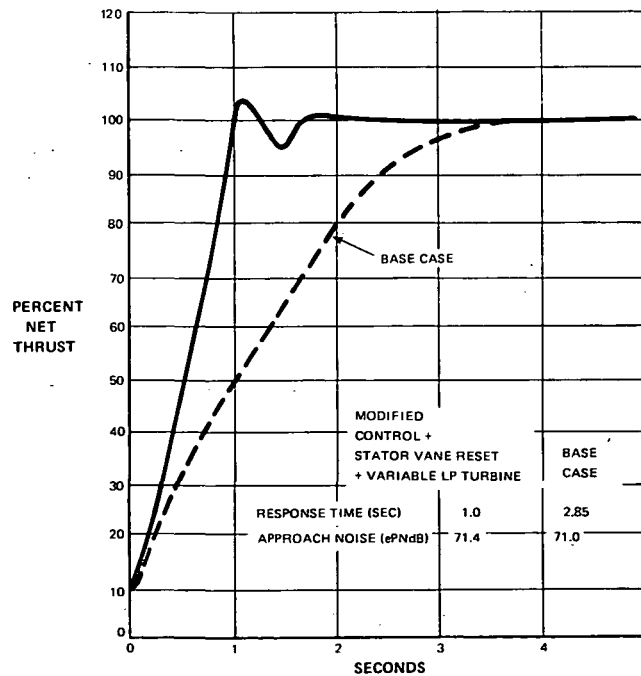


Figure 36 Combining Modified Control Logic, Stator Vane Reset and Variable Low Pressure Turbine Area  $\sim 6^\circ$  Approach

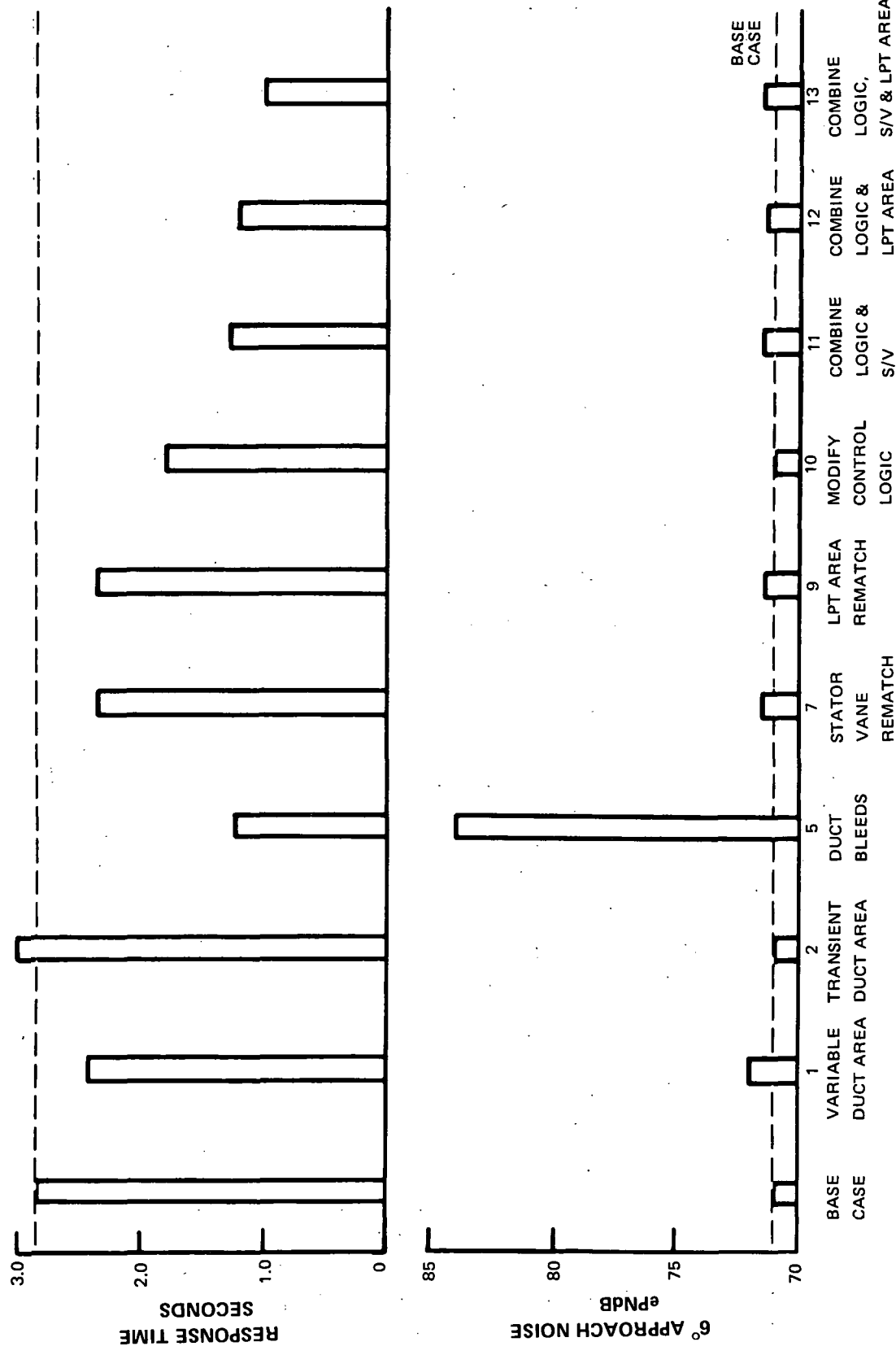


Figure 37 Summary of Promising Schemes

## CONCLUSIONS AND RECOMMENDATIONS

*The engine cycle selected for an Advanced Technology Transport (ATT) planned for commercial operation in the 1980's considered low noise as one of the major design criteria. Additional reduction in the community noise exposure can be realized by adopting noise abatement procedures during take-off and landings. Specifically, the use of steeper approach glide slopes during the landing maneuver will result in a significant reduction in the noise level. This report describes the studies performed to assure that the present levels of air transport safety are not compromised by using a steeper glide slope approach.*

*The study had two objectives; to evaluate the engine thrust response requirements necessary to establish a positive climb gradient from an aborted landing approach at various glide slope angles, and, to investigate various methods of achieving rapid thrust response during the go-around maneuver.*

*It was determined that steeper glide slopes require less stringent engine response as a result of the longer time necessary to rotate the aircraft to a positive climb gradient without exceeding the maximum allowable angle of attack. This demonstrates the dependence of the thrust response requirements on the aerodynamic capability of the aircraft and its ability to respond to control inputs. To substantiate these preliminary results, it is recommended a real time computer simulation of the aircraft response characteristics be conducted.*

*Improved engine response is obtainable by careful design of the fuel control functions to take full advantage of the acceleration capability of the engine. These functions cannot be easily implemented with conventional hydromechanical techniques; instead, a full-authority electronic control system will be necessary. Resetting the compressor stator vanes during the approach provides additional thrust response during the acceleration from an aborted landing. This is obtainable with negligible increase in cost, weight or approach noise. A program to demonstrate rapid response schemes with Pratt & Whitney Aircraft's "Real Time Control Simulator" on an existing production engine is recommended.*

*The steeper glide slope approach appears to be an attractive method of reducing the community noise level without penalizing the performance and safety aspects of the aircraft.*

## LIST OF SYMBOLS

$C_{MAC}$	Pitching moment coefficient
$\bar{C}$	Mean aerodynamic chord $\sim$ ft (m)
$D$	Drag force $\sim$ lbs (N)
$g$	Acceleration due to gravity $\sim$ ft/sec <sup>2</sup> (m/sec <sup>2</sup> )
$I_{zz}$	Moment of Inertia
$L$	Lift force $\sim$ lbs (N)
$l$	Moment arm $\sim$ ft (m)
$MAC$	Moment about the aerodynamic center
$q$	Dynamic Pressure = $\frac{1}{2} \rho V^2 \sim$ lb/ft <sup>2</sup> (N/m <sup>2</sup> )
$S$	Area - ft <sup>2</sup> (m <sup>2</sup> )
$V$	Velocity $\sim$ ft/sec (m/sec)
$W$	Weight $\sim$ lbs (kg)
$\alpha$	Angle of attack
$\gamma$	Flightpath angle
$\delta$	Elevator deflection angle $\sim$ degrees
$\phi$	Attitude of the aircraft
$\frac{\partial C_L}{\partial \alpha}$	Rate of change of lift coefficient with respect to change of angle of attack
$\frac{\partial C_L}{\partial \delta}$	Rate of change of lift coefficient with respect to change of elevator deflection
$\frac{d}{dt}$	Rate of change with respect to time
$\frac{d^2}{dt^2}$	Acceleration

## LIST OF SYMBOLS (Cont'd)

$N_2$	High Rotor Speed, rpm
$N_1$	Low Rotor Speed, rpm
$A_{jd}$	Duct Nozzle Area, ft <sup>2</sup> (m <sup>2</sup> )
$A_{je}$	Primary Nozzle Area, ft <sup>2</sup> (m <sup>2</sup> )
PLA	Powers Lever Angle
$W_f$	Fuel Flow, lb/sec (kg/sec)
$P_b$	Burner Pressure, psia (N/m <sup>2</sup> )
CET	Combustor Exit Temperature, °F (°C)
$F_n$	Engine Net Thrust, lbs (N)

## Subscripts

( ) <sub>ELEV</sub>	Elevator
( ) <sub>STAB</sub>	Stabilizer

# DISTRIBUTION LIST

	Copies		Copies
National Aeronautics and Space Administration		Mr. L. M. Wenzel, MS: 100-1	1
Washington, DC 20546		Mr. N. T. Musial, MS: 500-311	1
		Library, MS: 60-3	2
Code R, Mr. Roy P. Jackson	1	Report Control Office, MS: 5-5	1
Code RD-M, Mr. Edwin C. Kilgore	1		
Code RD-P, Mr. George W. Cherry	1	National Aeronautics and Space Administration	
Code RD-T, Dr. Seymour C. Himmel	1	Flight Research Center	
Code RG, Mr. Gerald G. Kayten	2	P. O. Box 273	
Code RH, Mr. Albert J. Evans	1	Edwards, CA 93523	
Code RA, Mr. William S. Aiken	1		
Code RL, Mr. Harry W. Johnson	2	Mr. Lee R. Scherer, Director, Code C	1
Code RW, Mr. George C. Deutsch	1	Mr. D. A. Deets, Code R	1
Code RE, Mr. Frank J. Sullivan	1		
Code RX, Mr. Richard J. Wisniewski	1	National Aeronautics and Space Administration	
		Langley Research Center	
National Aeronautics and Space Administration		Hampton, VA 23365	
Ames Research Center			
Moffett Field, CA 94035		E. M. Cortright, Director, MS: 106	1
		O. W. Nicks, Deputy Director, MS: 103	1
Code D, Dr. Hans M. Mark	1	Dr. J. E. Duberg, Assoc. Dir., MS: 103	1
Code FAV, Mr. Rodney O. Bailey	1	R. E. Bower, MS: 116	1
		T. A. Toll, MS: 249-A	12
National Aeronautics and Space Administration		W. J. Alford, Jr., MS: 249-A	1
Lewis Research Center			
21000 Brookpark Road		Air Transport Association of America	
Cleveland, OH 44135		1000 Connecticut Avenue, NW	
		Washington, DC 20036	
Mr. B. T. Lundin, Director, MS: 3-2	1		
Dr. B. Lubarsky, MS: 3-3	1	Vern W. Ballenger	1
Mr. M. A. Beheim, MS: 86-1	1		
Mr. W. L. Stewart, MS: 501-5	1	Department of Transportation	
Mr. R. W. Schroeder, MS: 501-5	1	Federal Aviation Administration	
Mr. J. H. Povolny, MS: 60-6	1	Washington, DC 20590	
Mr. E. W. Conrad, MS: 501-4	1		
Mr. C. C. Ciepluch, MS: 501-4	1	George P. Bates, Jr., Code RD-700	1
Mr. D. N. Bowditch, MS: 86-1	1		
Mr. R. J. Weber, MS: 86-1	1	Grumman Aerospace Corporation	
Dr. E. J. Rice, MS: 501-5	1	South Oyster Bay Road	
Mr. J. F. Dugan, Jr., MS: 86-1	1	Bethpage, Long Island, NY 11714	
Mr. A. J. Glassman, MS: 77-2	1		
Mr. R. R. Secunde, MS: 500-202	1	Mark H. Siegel, Dept. 391, Plant 30	1
Mr. R. J. Rulis, MS: 501-2	1		
Mr. A. A. Medeiros, MS: 501-4	1	Headquarters	
Mr. M. J. Hartmann, MS: 5-9	1	United States Air Force	
Mr. S. S. Manson, MS: 49-1	1	Washington, DC 20330	
Mr. J. B. Esgar, MS: 60-4	1		
Mr. L. W. Schopen, MS: 500-206	1	Lt. Col. Robert H. Blinn, Jr., AFRDQ	1
Mr. R. J. Antl, MS: 501-4	43		

# DISTRIBUTION LIST (Cont'd)

	Copies		Copies
Department of the Air Force AFML Wright-Patterson Air Force Base, OH 45433		American Air Lines, Inc. 633 Third Avenue New York, NY 10017	
Bernard Chasman	1	M. B. Fannon	1
Department of the Air Force AFFDL Wright-Patterson Air Force Base, OH 45433		Pan American World Airways, Inc. Pan Am Building New York, NY 10017	
Maj. Joseph E. Graetch	1	William F. Hibbs	1
Lawrence Kummeth	1	Wright-Patterson Air Force Base	
Cecil Wallace	1	AFAPL/TBP	
Secretary of the Air Force/SAFRDD Washington, DC 20330		Wright-Patterson Air Force Base, OH 45433	
Laurence K. Loftin, Jr.	1	L. J. Obéry	1
Department of the Air Force AFAPL Wright-Patterson Air Force Base, OH 45433		Eastern Air Lines, Inc. Miami International Airport Miami, FL 33148	
George E. Thompson	1	James E. McMillen	1
Department of the Navy Naval Air Systems Command Washington, DC 20360		Delta Airlines Atlanta Airport Atlanta, GA 30320	
James C. Taylor, Code AIR 530141C	1	W. J. Overend	1
Trans World Airlines, Inc. 605 Third Avenue New York, NY 10016		Gates Learjet Corporation P. O. Box 1280 Wichita, KS 67201	
Edward A. Carroll	1	Ronald D. Neal	1
United Air Lines, Inc. San Francisco International Airport San Francisco, CA 94128		National Aeronautics and Space Council Executive Office of the President Washington, DC 20502	
Richard E. Coykendall	1	Richard D. Fitzsimmons	1
United Air Lines, Inc. P. O. Box 66100 Chicago, IL 60666		Department of Transportation Office of Secretary of Transportation Washington, DC 20590	
Harry G. Lehr	1	Lawrence P. Greene, Code TST-22	1



## DISTRIBUTION LIST (Cont'd)

	Copies		Copies
Department of Transportation Joint DOT/NASA Noise Abatement Office Washington, DC 20590		Mr. S. M. Nehez Deputy for Development Planning Aeronautics System Division Directorate for General Purpose and Airlift Systems Planning (XRL) Wright-Patterson Air Force Base, OH 45433	
Louis J. Williams, Code TST-53	1		1
McDonnell-Douglas Corporation 3855 Lakewood Boulevard Long Beach, CA 90801		Department of the Air Force AFSC Wright-Patterson Air Force Base, OH 45433	
Edward S. Rutowski	1		
North American Rockwell Corporation 4300 East 5th Avenue Columbus, OH 43216		Col. Francis J. McNamara, Jr.	1
Reid B. Lyford	1	Lt. Col. Alan M. Edwards Executive Office of the President National Aeronautics and Space Council Washington, DC 20502	1
William E. Palmer	1		
Bell Aerospace Company Buffalo, NY 14240		Boeing Commercial Airplane Company A Division of The Boeing Company P. O. Box 3707 Seattle, WA 98124	
Alan Coles	1		
LTV Aerospace Corporation Vought Missiles and Space Company 3221 North Armistead Avenue Hampton, VA 23366		Glen W. Hanks, Advanced Transport Technology, MS: 4139	1
Charles W. Pearce	1	Lockheed-California Company Dept. 74-31 Plant 2, Bldg. 202 P. O. Box 551 Burbank, CA 91503	
Northrop Corporation 1800 Century Park East Century City Los Angeles, CA 90067		T. Sedjwick	1
Sidney A. Powers	1	General Dynamics Corporation Convair Aerospace Division P. O. Box 748 Fort Worth, TX 76101	
Joint DOT/NASA CARD Implementation Office 400 7th Street, SW Washington, DC 20590		A. J. K. Carline	1
William N. Gardner, Code TST-31	1	Lockheed-Georgia Company 86 South Cobb Drive Marietta, GA 30060	
		R. H. Lange, Zone 401, Dept. D/72-79	1

## DISTRIBUTION LIST (Cont'd)

	Copies	Copies
Mr. C. J. Schueler, Chief Aerodynamics Division von Karman Gas Dynamics Facility Arnold Research Organization, Inc. Arnold Air Force Station, TN 37389	1	
NASA Scientific and Technical Information Facility P. O. Box 33 College Park, MD 20740		
Attn: Acquisitions Branch	10	